Charles University in Prague

Faculty of Science

Study program: Chemistry

Branch of study: Organic chemistry

Bc. Elena Shcherbachenko

Reakční intermediáty v homogenní zlatné katalýze.

Reaction intermediates in homogeneous gold catalysis.

Master thesis

Supervisor: prof. Mgr. Jana Roithová, Ph.D.

Praha, 2016

Prohlášení

Prohlašuji, že jsem závěrečnou práci zpracovala samostatně a že jsem uvedla všechny použité informační zdroje a literaturu. Tato práce ani její podstatná část nebyla předložena k získání jiného nebo stejného akademického titulu.

V Praze dne 5. května 2016

Podpis

Elena Shcherbachenko

Statement

I declare that I prepared the diploma thesis individually and that I properly cited all used information and literary sources. Neither this work nor substantial part of this work was submitted in order to obtain another or the same academic degree.

In Prague 5. 05. 2016

Signature

Elena Shcherbachenko

Acknowledgment

First of all, I would like to thank my supervisor Prof. Jana Roithová for the opportunity to work in this group and for an interesting subject for the master thesis. Secondly, I would like to thank RNDr. Simona Hybelbauerová, Ph.D. for measuring of nuclear magnetic resonance spectra. I also would like to thank all other members of our research group for advices and friendly atmosphere.

Abstrakt

Předkladáná diplomová práce je zaměřena na výzkum reakčních intermediátů v reakcích katalyzovaných homogenními zlatnými katalyzátory. Hlavní experimentalní technikou je hmotnostní spektrometrie spojená s elektrospejovou ionizací (ESI-MS). Zpožděné značení reaktantu bylo použito jako hlavní metoda. Zaměřila jsem se na výzkum hydratace 1-fenyl-1propynu zlatným komplexem [Au(IPr)(MeCN)]BF_4 (IPr = 1,3-Bis(2,6-di-iso-propylfenyl)imidazol-2-yliden).

Detekovala jsem dva hlavní intermediáty obsahující jeden nebo dva atomy zlata (monoaurovaný a diaurovaný intermediát). Získala jsem rychlostní konstanty jejich rozpadu a poločasy jejich života. Odvodila jsem kinetické isotopické efekty pro rozpad a vznik detekovaných reakčních intermediátů. Ukázala jsem, že kinetika spojená s jejich rozpadem je identická, což naznačuje, že hydratace alkynů katalyzovaná zlatným komplexem [Au(IPr)(MeCN)]BF_4 pravděpodobně probíhá přes neutralní monoaurované intermediáty, které detekuji pomocí protonace (monoaurovaný intermediát) nebo pomocí komplexace s druhým kationtem zlata (diaurovaný intermediát).

Klíčová slova: *zlatná katalýza, reakční intermediáty, elektrosprejová ionizace, hmotnostní spektrometrie.*

Abstract

The presented master thesis is devoted to the investigation of reaction intermediates in homogeneous gold catalysis. Electrospray ionization mass spectrometry (ESI-MS) was used as the primary research technique in this study. Delayed reactant labeling was used as the main method. I have focused mainly on the hydration of 1-phenyl-1-propyne catalyzed by the gold complex [Au(IPr)(MeCN)]BF_4 (IPr = 1,3-bis(2,6-di-iso-propylphenyl)imidazol-2-ylidene).

I have detected two main intermediates containing one or two gold atoms, respectively (monoaurated and diaurated intermediate). I have obtained rate constants for the degradation of the reaction intermediates and their half-lives. I have derived kinetic isotope effects for the formation and the decomposition of the detected intermediates. I have shown that the kinetics of the degradation of both intermediates is identical, therefore I conclude that hydration of alkynes catalyzed by gold complex [Au(IPr)(MeCN)]BF_4 proceeds most probably via neutral monoaurated intermediates. These neutral intermediates are detected by ESI-MS as protonated (monoaurated intermediate) or tagged by a second gold cation (diaurated intermediate).

Key words: *gold catalysis, reaction intermediates, electrospray ionization, mass spectrometry.*

List of abbreviations

CID	collision induced dissociation
ESI	electrospray ionization
IPr	1,3-Bis(2,6-di-iso-propylphenyl)imidazol-2-yliden
IRMPD	infrared multiphoton dissociation
KIE	kinetic isotope effect
MS	mass spectrometry
NMR	nuclear magnetic resonance
ROMP	ring-opening metathesis polymerization

Contents

1 Introduction

Gold catalysis is an innovative area in catalysis research. The ability of gold catalysts to provide high selective, atom-economic transformations lead to an expansion of its utilization.[1] Homogeneous gold-catalyzed reactions proceed in multistep mechanism and it is a challenge for chemists to uncover it. Solid information can be obtained by detection and investigation of the reaction intermediates.[2, 3]

A powerful tool for the investigation of reaction intermediates is electrospray ionization mass spectrometry.[4] Its big advantage is its sensitivity, since reaction intermediates are present in the mixture in very low concentrations. ESI-MS works directly from dilute solution, provide us access to the structure, bond energies and even kinetic data for reaction intermediates.

Due to the new method, referred to as delayed reactant labeling, we can obtain rate constants for the degradation of reaction intermediates and investigate the effects of reaction conditions on their half-life.[5] In association with data obtained from nuclear magnetic resonance (NMR) experiments and from theoretical calculations, this method can lead us to new insights on the reaction mechanism.

2 Aims of the thesis

- to detect the reaction intermediates for the chosen reaction by ESI-MS
- to determine the rate constants for the degradation of the detected intermediates and their half-lives using delayed reactant labeling method
- to derive kinetic isotope effects for the degradation of the intermediates
- to use the obtained results for discussion about the reaction mechanism of given reaction

3 Theoretical background and review of current literature

3.1 Gold catalysis

Gold compounds were considered inert catalytic species for a long time. The inertness of elemental gold and its high cost were reasons why was this metal overlooked in catalytic research for a long time. However, in the nineties it was discovered, that gold salts and complexes are highly catalytically active species. In addition, a combination of factors led to a lower and stable price of gold in comparison with other metals that are used even in large-scale technical catalysis processes like rhodium, palladium, and platinum.[6]

Exceptional Lewis acidity of gold species is utilized in the major part of gold-catalyzed reactions. Due to the relativistic effects gold(I) complexes are extremely soft Lewis acids and react preferentially with soft nucleophiles such as π C-C bonds.[7] Gold complexes do not switch between oxidation states without an additional oxidant, but gold(III) complexes are easily accessible and also find catalytic applications (scheme 3.1).[8,9]

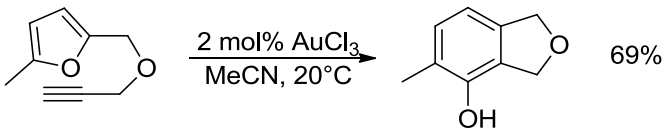

Scheme 3.1. Intramolecular phenol synthesis catalyzed by $AuCl_3$.[6]

Gold(III) complexes are harder Lewis acids then gold(I) and show a larger oxophilic character. The synthesis of halofuranes may serve as an example of the different behavior of Au(III) and Au(I) compounds (Scheme 3.2). The oxophilic Au(III) species coordinates to the oxygen atom and induces intramolecular Michael addition of Br to the enone. The obtained bromoirenium zwitterion yields in a cyclization step 3-bromofuran. On the contrary, slightly more π-philic Au(I) species coordinates to the double bond of the allene, and catalyzes the formation of 2-bromofuran.[10]

A significant part of gold catalysis research involves an addition of a nucleophile to triple bonds, catalyzed by gold.[11] Certainly, gold catalysts bring big advantages in the area of alkynes hydration.[12,13] Gold-catalyzed hydration of alkynes carried out under mild conditions[14] gives high yields with low catalytic loading,[15] hydroalkoxylation can be even stereoselective.[16]

3.1.1 Gold catalysts in the addition of water and alcohols to alkynes

First note about the catalytic activity of gold in addition of water to alkynes appeared in 1898.[8] In this paper authors described the synthesis of acetaldehyde from acetylene with a mercury sulfate as the catalyst. They also described the reaction of acetylene with aqueous solutions of metal salts, one of these salts was gold(III) chloride. The observation of gold catalytic activity was then completely unnoticed.[17]

Several other reports describe the use of $NaAuCl_4$ as a catalyst for the addition of water and methanol to nonactivated alkynes, but this catalyst is quickly reduced to inactive metallic gold.[18]

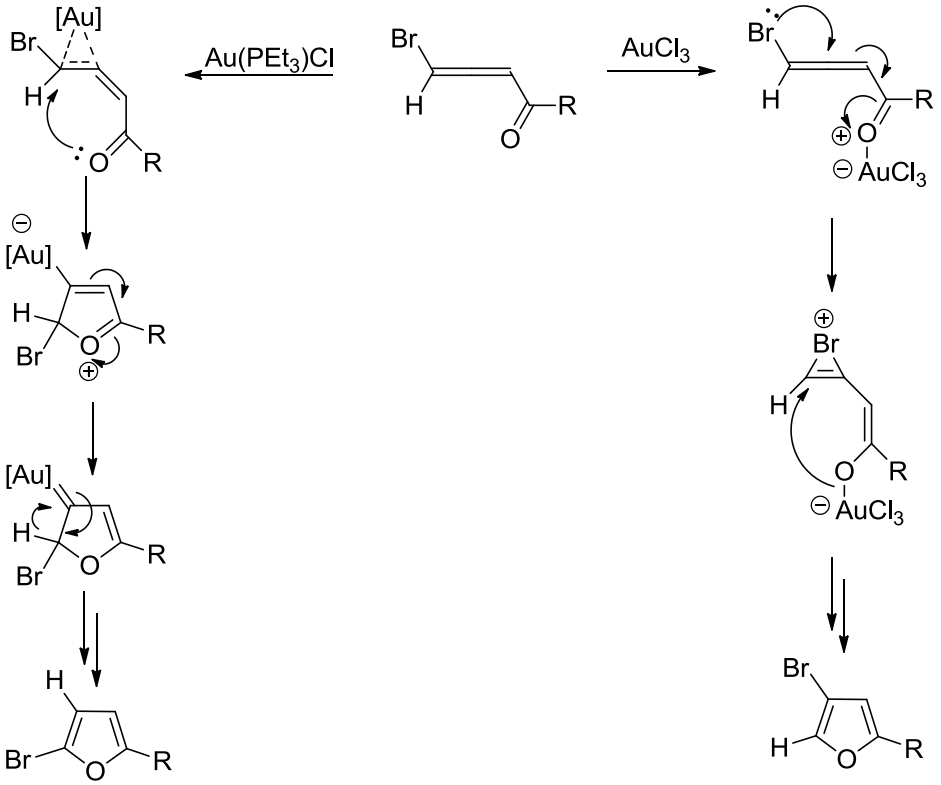

Scheme 3.2. Two pathways to selective formation of 2- and 3-bromofuranes, R = C_8H_{17}.[10]

In 1998, Teles and co-workers published a paper where the addition of alcohols to alkynes was catalyzed by gold in a presence of acid as cocatalyst. With the cationic gold complexes of the general type [L-Au^+] (where L is phosphine, arsine or phosphite) they achieved high turnover numbers, up to 10^5 moles of product per mole of catalyst. They

also proposed a mechanism for the addition of methanol to propyne catalyzed by $[Au(PMe_3)]^+$ (scheme 3.3).[19]

In the first step, gold cation coordinates to the triple bond of propyne. This step is generally accepted as a first step for the most of the gold catalyzed reactions where a multiple CC bond is activated.[2,20,21,22] Coordination of methanol to gold was proposed to lead to the nucleophilic attack of methanol to the triple bond to form vinyl gold complex **3-1**. Then intermediate **3-2** is supposed to be formed by 1,3-hydrogen migration or deprotonation at the oxygen atom and reprotonation at the carbon atom. The last step is deauration leading to the product and to the catalyst regeneration.

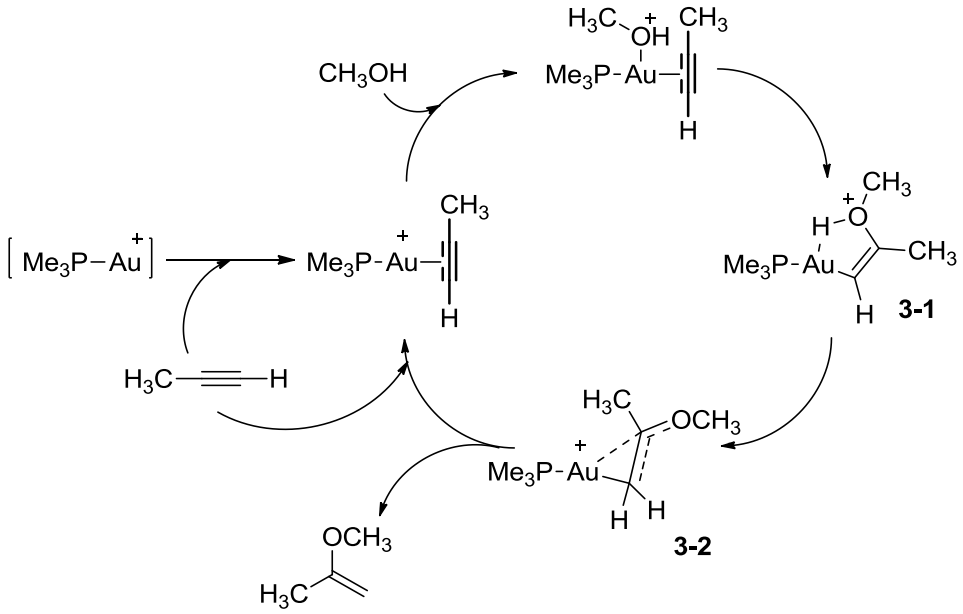

Scheme 3.3. Mechanism for the addition of methanol to propyne catalyzed by $[Au(PMe_3)]^+$ Proposed by Teles and co-workers.[19]

In 2012 Roithová and co-workers suggested, based on kinetic studies and theoretical calculations, that the addition of methanol to a triple bond proceeds with a dual activation mechanism.[23] They proposed that methanol is added to the gold-activated triple bond of an alkyne, in a form of gold methoxide. That led to the formation of *gem*-diaurated intermediates (Scheme 3.4).

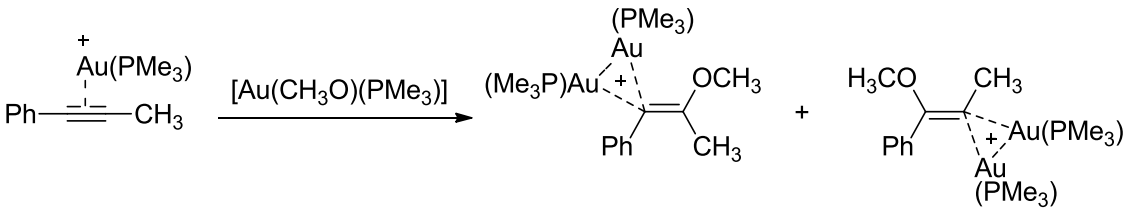

Scheme 3.4. Formation of *gem*-diaurated intermediates in the gold(I)-mediated reaction between an internal alkyne and methanol.[23]

Dual activation mechanism in addition of the methanol to alkynes was also suggested by Nolan and co-workers.[24] They used dinuclear gold complex **3-3** as a catalyst for the addition of differently substituted phenols to alkynes. They found out, that complex **3-3** decays to Lewis acid **3-4** and Brønsted base **3-5**. Generated complexes then independently react with alkyne and alcohol (scheme 3.5).

In 2014 Maier and Zhdanko published a paper, in which they suggested, that diaurated intermediates are undesired off-cycle products of the gold-catalyzed reaction of an alkyne with alcohol and just one gold center is required for the catalytic cycle (scheme 3.6).[25]

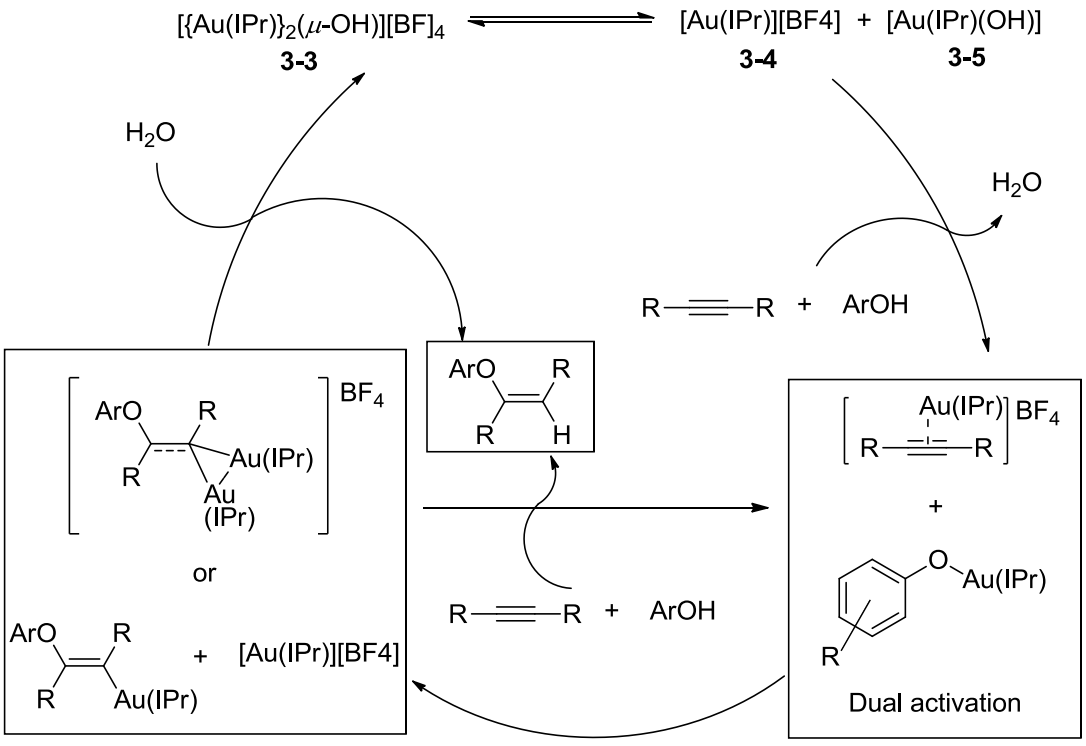

Scheme 3.5. Dual activation mechanism proposed by Nolan and co-workers.[24]

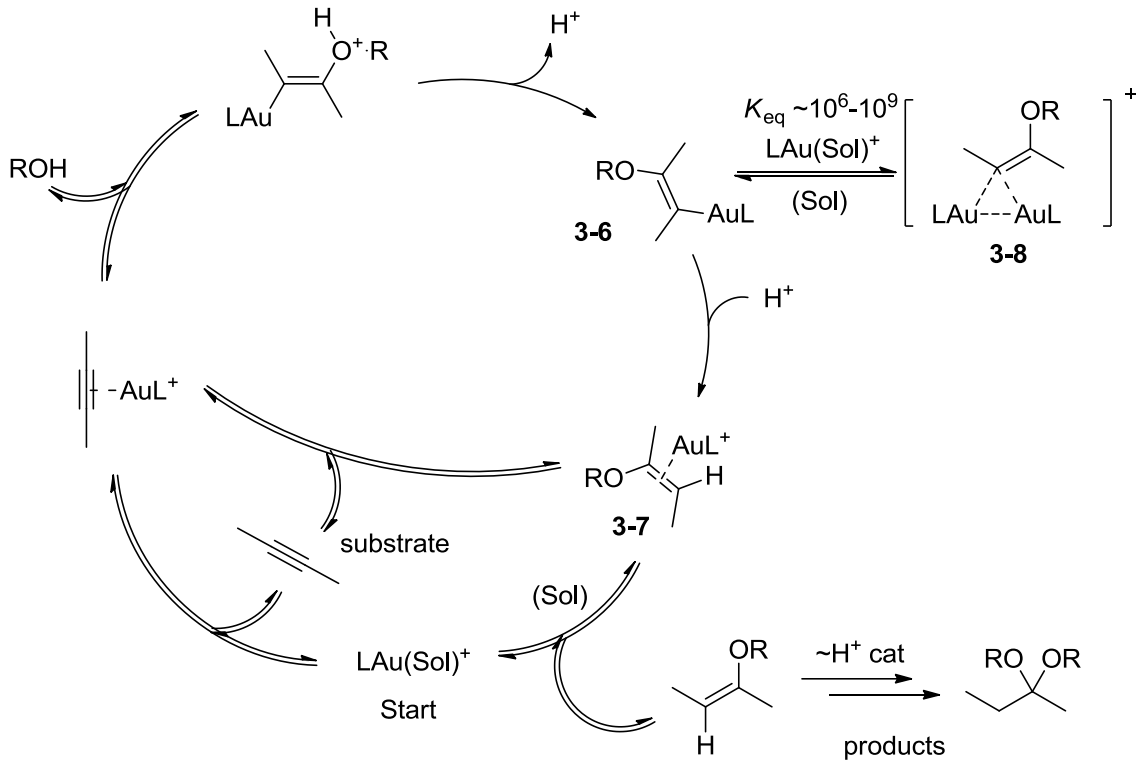

Shceme 3.6. Mechanism proposed by Maier and Zhdanko.[25]

They discovered, that **3-6** is a highly reactive intermediate, that undergoes protonolysis to give **3-7** cation or auration to give **3-8**. Formation of **3-8** is thermodynamically highly favored and **3-8** cannot undergo direct protodeauration. Thus, gold centers are caught in these species and cannot be return to the catalytic cycle.

The mechanism of the addition of methanol to an alkyne was further studied in the Roithová laboratory.[5] They used delayed reactant labeling method, theoretical calculations, and NMR studies to propose the following mechanism (scheme 3.7).

In their experiments they used two types of ligands: a bulky *N*-heterocyclic carbene ligand IPr (1,3-bis(2,6-diisopropylphenyl)imidazol-2-ylidene) and phosphine ligand PPh_3. They suggested, that in the case of the gold catalyst bearing a phosphine ligand diaurated intermediates are formed during the catalytic cycle. The first endothermic reversible step is the addition of methanol to a gold-activated alkyne. The next step is an exchange of the proton at the oxygen atom by a gold cation, this step leads to the diaurated intermediates **3-9**. This step is strongly exothermic and it is the driving force of the reaction. The rate–determining step is the protodeauration of diaurated intermediates (scheme 3.8).

In the case of the gold catalyst bearing bulky IPr ligand, the reaction goes through monoaurated intermediates **3-10**, which are formed by deprotonation of **3-11** (scheme 3.7). Recent studies of Zhdanko and Mayer showed that this step is probably mediated by counter ions present in the reaction mixture.[26] The overall reaction rate in the case of the gold catalyst bearing bulky IPr ligand is higher because of easier protodeauration of the monoaurated intermediate **3-10** in comparison to the protodeauration of diaurated intermediates **3-9.**

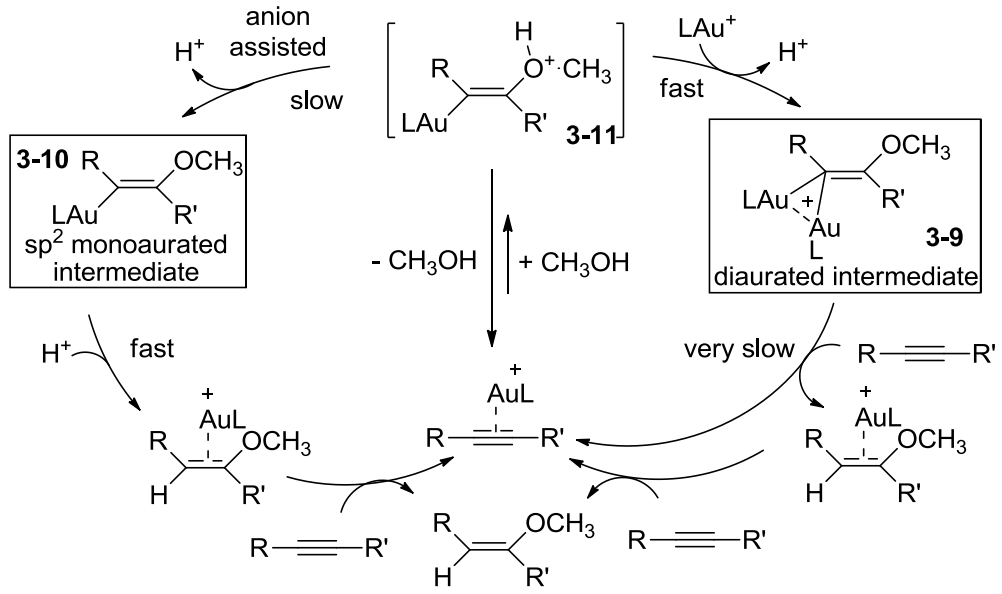

Scheme 3.7. Mechanism of the addition of methanol to an alkyne catalyzed by gold proposed by Jašíková and co-workers.[5] L = PPh_3 for the right path, L = IPr for the left path.[5]

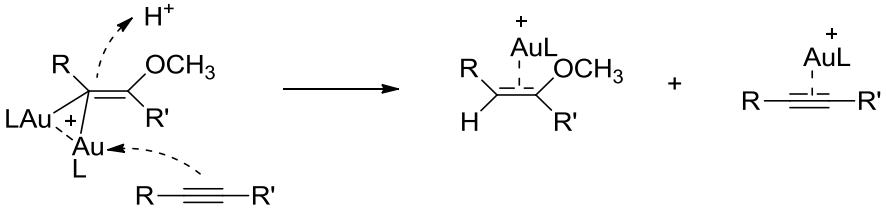

Scheme 3.8. Protodeauration of diaurated intermediates.[5]

In 2016 Gomez-Suarez and co-workers published a paper in which they investigated the mechanistic aspects of the dual gold-catalyzed hydrophenoxylation of alkynes by experimental and theoretical methods.[27] They suggested the dual activation mechanism for this reaction (scheme 3.9). Digold–phenoxide species **3-12** serve as precursors for

active catalytic species. *Gem*-diaurated species **3-13** were shown to be off-cycle species. Their formation during the reaction is unlikable, due the competing process mediated by water. *Gem*-diaurated species **3-13** are also unlikely to assist productive catalysis, because they lie in a very deep potential energy well.

Recently, two studies investigating the gold-catalyzed hydration of alkynes have been published.[28,29] In both works researches came to the same conclusions with regards to the ligand effect in the gold-catalyzed hydration of alkynes. According to them, electronic effects of the ligand played only a small role in the kinetics of alkyne hydration. A crucial role has been taken by steric properties of the ligands, bulkier ligands facilitates the reaction.

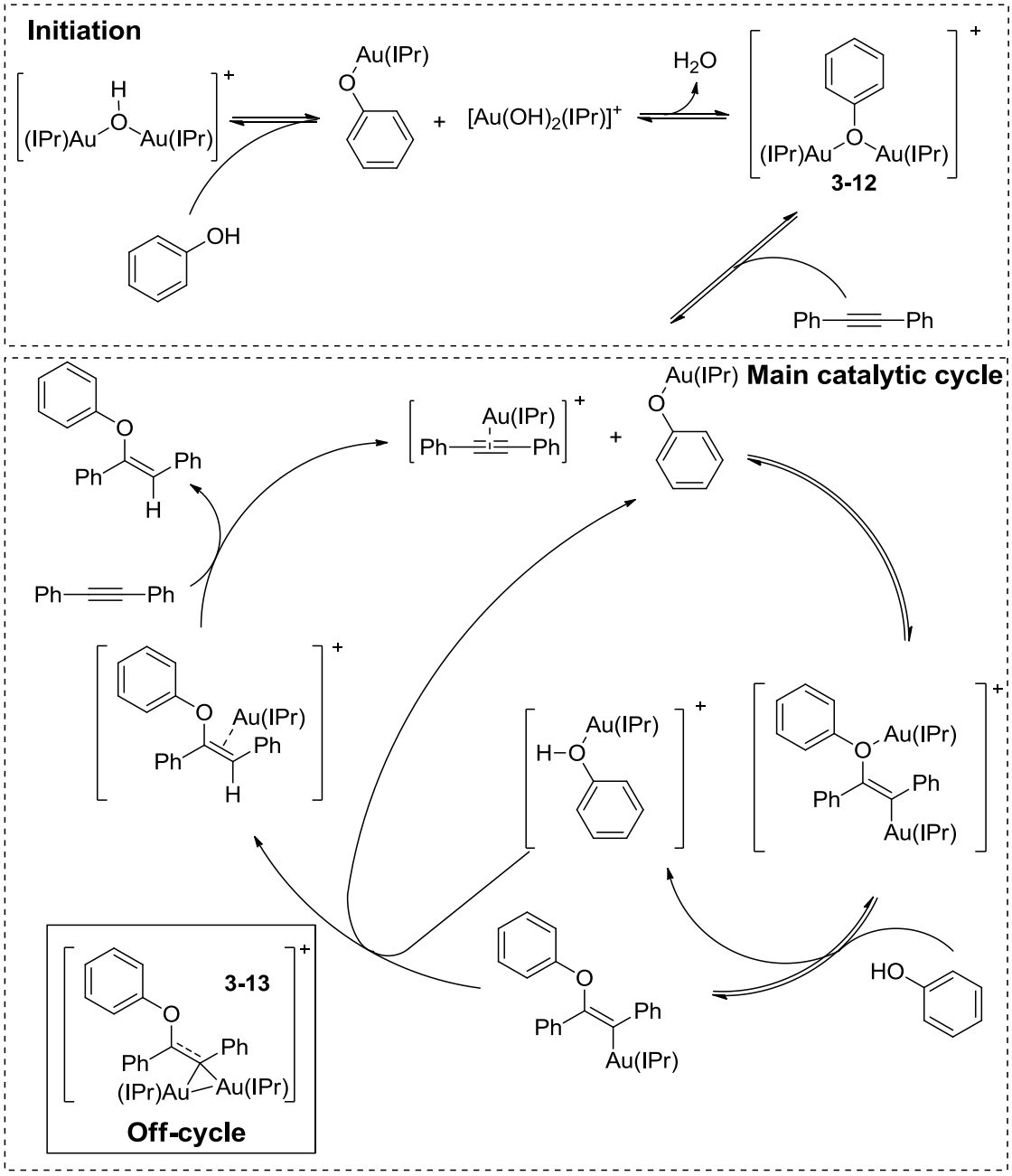

Scheme 3.9. Hydrophenoxylation of alkynes by dual gold activation catalysis. Mechanism, proposed by Gomez-Suarez and co-workers.[27]

The counterion effect also has been extensively studied. Several studies describe the counterion effect in the gold(I)-catalyzed hydroalkoxylations and alkoxylations of alkynes.[30,26,31] The total ion effect depends on the cooperation of several factors and can be theoretically described in every step of the reaction mechanism (scheme 3.10). In step I, anion holds the molecule of methanol at the right position for the nucleophilic attack and increases the nucleophilicity of methanol by the hydrogen-bond accepting properties. In protodeauration (step II) anion acts as a proton shuttle which decreases the energy barrier for this step. A strongly coordinating anion can deactivate the catalyst by blocking the alkyne coordination. In the case of a strongly basic anion, inactive alkoxide is formed.[31]

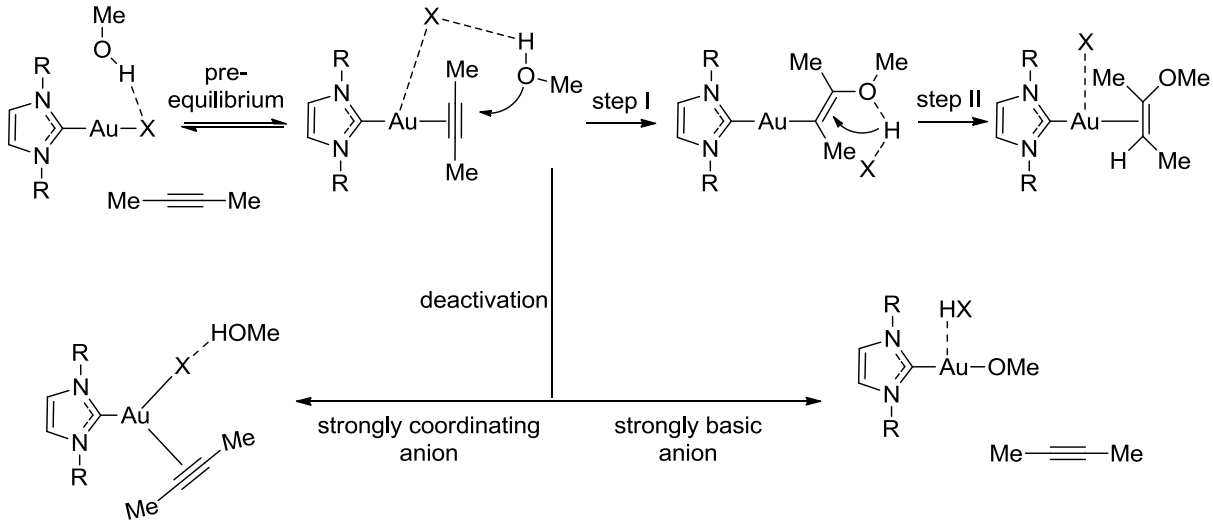

Scheme 3.10. The role of a counterion in the mechanism of the methanol addition to 2-butyne catalyzed by [NHCAuX].[31]

Regioselectivity of the gold-catalyzed hydration and hydroalkoxylation of alkynes also has been investigated. Regioselectivity of the specific reaction strongly depends on the type of the catalytic system, on the nucleophile and on the substituents of the alkyne.[32]

3.2 Electrospray ionization mass spectrometry (ESI-MS) in catalysis research

Electrospray ionization (ESI) is a technique used in mass spectrometry (MS) for a direct probing of liquid samples under gentle conditions.[33,34] ESI was developed by John Fenn for analysis of biological macromolecules. For his development, Prof. Fenn was awarded Nobel prize in 2002. This technique does not cause spontaneous ion fragmentation in most cases. It is as mild that it allows us, for example, to investigate non-covalent binding in organometallic complexes.[35] Due the high sensitivity of ESI-MS and high speed of detection of ions from the liquid sample, unstable intermediates in very small concentrations can be investigated.

ESI-MS can be used for online monitoring of reaction mixtures in a time range from several minutes to hours. The individual ions can be mass-selected and probed in collision-induced dissociation experiments (CID). From fragments, obtained by the CID experiments, ion structure can be determined. Energy-dependent CID experiments can also provide information about bond energies.[36,37,38,39,40]

ESI-MS is especially useful for investigations of reactions that involve ionic intermediates, thus ESI-MS is widely used in organometallic chemistry studies. Pioneer studies using ESI-MS as a tool for investigation of the reaction intermediates were made by Peter Chen and co-workers.[41] As an example can serve their investigation of the ring-opening metathesis polymerization (ROMP) of nonbornene or hydrogenation catalyzed by rhodium complexes.[42,43]

Compounds, sensitive to air and hydrolysis, like cuprates, can be also studied with ESI-MS.[44] Special technique for transporting of extremely sensitive compounds to mass spectrometer was also developed.[45] For the study of reaction intermediates, which are stable only on low temperatures, cold-spray ionization technique was developed.[46]

ESI-MS has likewise found an application in investigations of intermediates in organocatalytic reaction. Intermediates in those reactions can be charged or easily protonated by protic solvents.[47] Neutral intermediates also might be investigated, using the charge-tagging technology or by adding a little amount of alkali salt to the reaction mixture.[48,49]

Fundamental question in using ESI-MS for research is the correlation between solution and the gas phase.[50] Evaporation of solvent from the drops during the ESI process causes changes in concentration, solvation, pH of the solution.[51,52] Electrochemical processes in

ESI and ionization conditions should be also taken into account. Results can be also affected by the acceleration of reactions in charged droplets. Despite all possible complications, ESI-MS gives us useful insights to the reactions in solution. The best way of using ESI-MS in research is to combine ESI-MS with other methods (NMR, electrochemistry, infrared spectroscopy, infrared multiphoton dissociation spectroscopy (IRMPD), etc.) for correct interpretation of results.

4 Methods

4.1 Delayed reactant labeling

One of the drawbacks of the ESI-MS is that intensity of the peak in the spectrum does not correlate with the ion concentration in solution. We can bypass this disadvantage by using isotopically labeled internal standard.[53] In the research of reaction mechanism, we are interested in reactive intermediates. Clearly, the possibility of using a stable isotopically labeled standard does not apply here and the evolution of the concentration has to be monitored indirectly.

The new method for reaction intermediates investigation was developed by our team.[5] This method is referred to as a delayed reactant labeling and is based on the monitoring of the reaction mixture that contains one of the reactants as a mixture of isotopically labeled and unlabeled molecules in time. In mass spectrum we can see a couple of peaks that contain reactant. One of these peaks contains labeled reactant, the other peak contains unlabeled reactant. The key trick is the time delay (t_d) for adding the labeled reactant to the reaction mixture. That allows us to follow the kinetic of all ions that contain this particular reactant. We assume that the isotopic labeling does not affect the ionization effectivity. We evaluate the signals only relative to each other, thus overall intensity is not important.

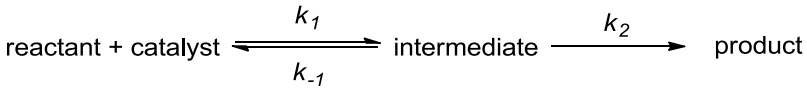

Scheme 4.1 Model reaction for kinetic model derivation.

A kinetic model for the mathematic description of the experimental data was derived from model shown in scheme 4.1. Here we assume first-order reaction between a reactant (R) and a catalyst (C) yielding an intermediate (I), which then converts into a product (P). If formation and destruction of the intermediate (I) can be described using steady-state approximation, then we can assemble following equation:

$$k_1 \cdot [R] \cdot [C] = (k_{-1} + k_2) \cdot [I]_{eq}, \quad (4.1)$$

where $[I]_{eq}$ is the equilibrium concentration of the intermediate.

The reaction mixture is first prepared with unlabeled reactants and allowed to react for the t_d. During this time a certain concentration of intermediate $[I]_{eq}$ is achieved. After time delay a labeled reactant (R^{label}) is added and the system is deflected from the steady-state conditions. After adding a labeled reactant (R^{label}), reaction mixture is monitored by ESI-MS (figure 4.1).

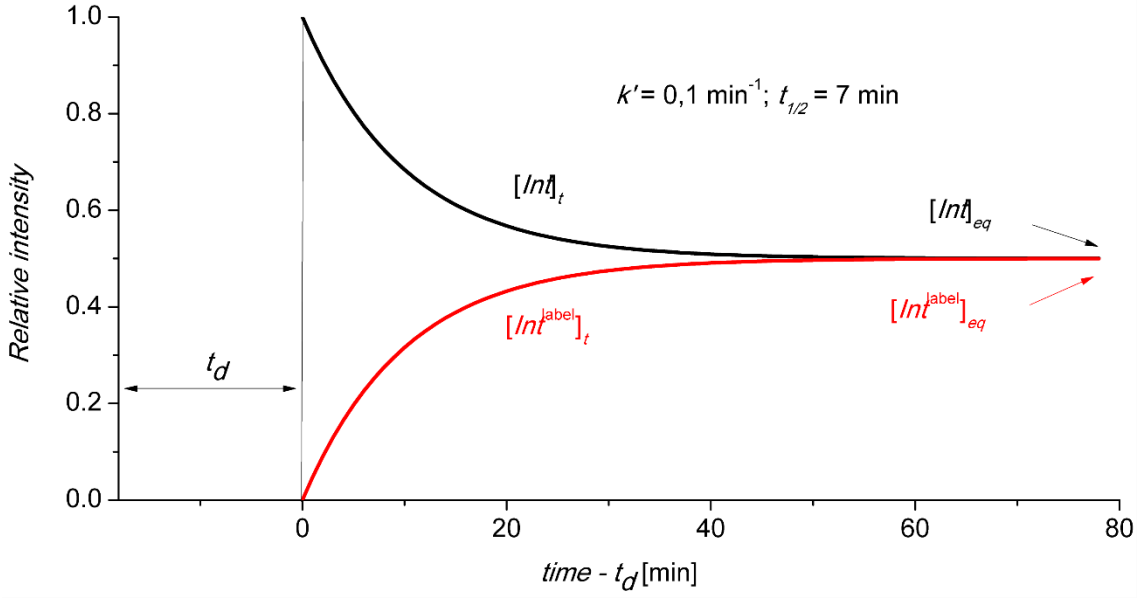

Figure 4.1. Ideal time evolution of the ESI-MS signals of unlabeled and labeled intermediates. The labeled intermediate was added to the reaction mixture with a time delay t_d. $[I]_{eq} = [I^{label}]_{eq} = 0,5$ for the given ideal experiment.

Evolution of the intensity of signals that corresponds to the reaction intermediate (I) and to the labeled intermediate (I^{label}) in time reflects reestablishment of the steady-state conditions and can be described by following equation:

$$\frac{d[I]}{dt} = (k_{-1} + k_2) \cdot [I]_{eqv} - (k_{-1} + k_2) \cdot [I] = k' \cdot ([I]_{eqv} - [I]), \qquad (4.2)$$

where $k' = k_{-1} + k_2$.

At the mixing time t_0 no labeled intermediate is present in the mixture ($[I^{label}] = 0$). If we normalize a sum of the concentrations of the labeled and unlabeled intermediate to one ($[I^{label}] + [I] = 1$), their time dependence (blue and red curves on figure 4.1) can be described by the following equations:

$$[I]_t = e^{-k't} + [I]_{eqv} \cdot (1 - e^{-k't}) \qquad (4.3)$$

$$[I^{label}]_t = [I^{label}]_{eqv} \cdot \left(1 - e^{-k't}\right). \quad (4.4)$$

In the real experiment precise ratio of the labeled and unlabeled intermediates is obtain by fitting experimental data. For half-lives of the intermediates the following equation can be used:

$$t_{1/2} = \frac{\ln 2}{k'}. \quad (4.5)$$

The rate of the formation of the intermediates (k_1) does not influence the shape of the curves if we assume, that the rate constant for formation of both, labeled and unlabeled intermediates is the same. Further we assume that the labeled and the unlabeled intermediates react with the same rate constant.

Usually, the setting up of a ESI-MS experiment takes around 1-3 minutes, thus if we want to determine a relevant rate constant the half-life of the intermediate cannot be too short. It does not matter whether labeled or unlabeled reactant is added first to the reaction mixture, we will obtain the same result by both approaches.

5 Results and discussion

I used electrospray ionization mass spectrometry (ESI-MS) and nuclear resonance spectroscopy (NMR) to study the addition of water to alkynes. I focused on the hydration of 1-phenyl-1-propyne catalyzed by gold complex [Au(IPr)(MeCN)]BF_4.

I used stock solutions in the preparation of reaction mixtures for experiments. Stock solution A contains catalyst [Au(IPr)(MeCN)]BF_4, solution B contains alkyne $PhCCCH_3$, solution C contains labeled alkyne $PhCCCD_3$. The exact composition of the stock solutions is given in table 6.1.

I started with the analysis of the source spectrum of the reaction mixture (figure 5.1). The reaction mixture was prepared by mixing 80 µl of the stock solution A, 120 µl of B and 100 µl of H_2O in 200µl of acetone.

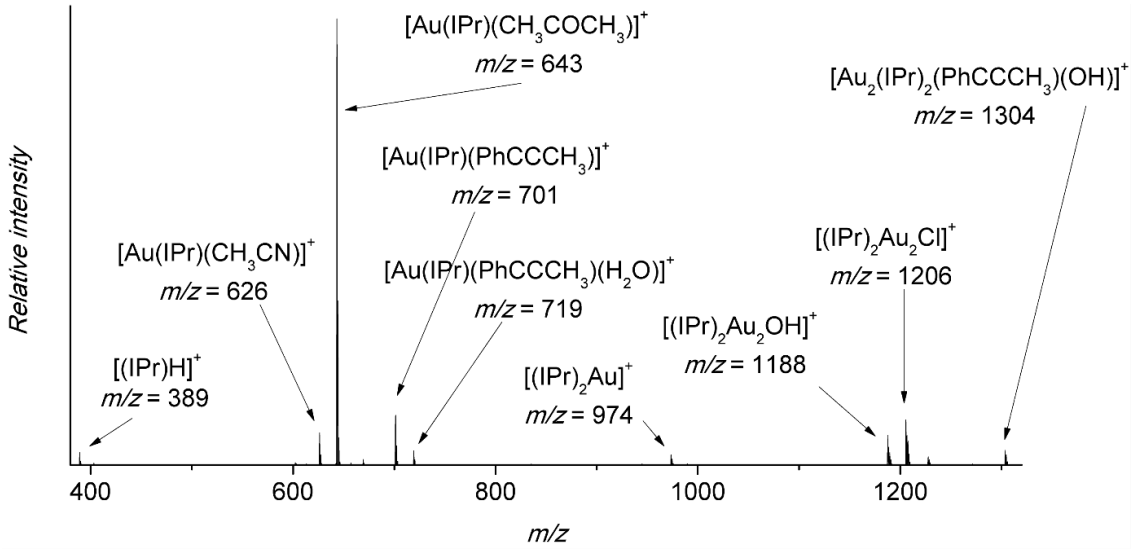

Figure 5.1. Source spectrum of the reaction mixture with unlabeled reactants.

Electrospray ionization of the reaction mixture led to several complexes of the catalyst with ions and molecules that are present in the reaction mixture ($[Au(IPr)(CH_3CN)]^+$, *m/z* = 626; $[Au(IPr)(CH_3COCH_3)]^+$, *m/z* = 643; $[(IPr)_2Au_2OH]^+$, *m/z* = 1188; $[(IPr)_2Au_2Cl]^+$, *m/z* = 1206). We can also see a significant amount of the ions $[(IPr)H]^+$ (*m/z* = 389) and $[(IPr)_2Au]^+$ (*m/z* = 974). Ions $[Au(IPr)(PhCCCH_3)]^+$ (*m/z* = 701), $[Au(IPr)(PhCCCH_3)(H_2O)]^+$ (*m/z* = 719), $[Au_2(IPr)_2(PhCCCH_3)(OH)]^+$ (*m/z* = 1304) contain reactant and can be a part of the catalytic cycle.

Using delayed reactant labeling method (chapter 4.1.1), I examined complexes $[Au(IPr)(PhCCCH_3)(H_2O)]^+$ and $[Au_2(IPr)_2(PhCCCH_3)(OH)]^+$.

5.1 Labeling with $PhCCCD_3$

a) Experiments with H_2O

Reaction mixtures were prepared by mixing 80 µl of the stock solution A, 120 µl of B and 100 µl of H_2O in 200µl of acetone and left to react for a time delay. After a time delay elapsed, 120 µl of solution C was added and reaction mixture was immediately monitored by ESI-MS. The time delay should not be too short, because a significant amount of the unlabeled intermediates must be formed. It also cannot be too long, because after a longer reaction time the obtained rate constants may be affected by other effects (catalyst degradation, the influence of minor products).

Three different time delays were tested: 30 minutes, 1 hour and 2 hours. The result of the experiment with 1 hour time delay is shown in figure 5.2. In the spectrum, recorded 2 minutes after the solution C was added, only a small amount of the labeled ions $[Au_2(IPr)_2(PhCCCD_3)(OH)]^+$ and $[Au(IPr)(PhCCCD_3)(H_2O)]^+$ can be observed (figure 5.2a). In the spectrum recorded 1 hour after the mixing (figure 5.2b), the ratio of the labeled ions $[Au_2(IPr)_2(PhCCCD_3)(OH)]^+$ and $[Au(IPr)(PhCCCD_3)(H_2O)]^+$ to unlabeled $[Au_2(IPr)_2(PhCCCH_3)(OH)]^+$ and $[Au(IPr)(PhCCCH_3)(H_2O)]^+$ is almost 1:1. The equilibrium for a π-complex between the catalyst and the alkyne (figure 5.2c) is achieved so fast that it cannot be followed by the current technique.

For the analysis, the sum of the signal intensities of the labeled and the unlabeled ions was normalized to 1. Time dependence of these normalized intensities was fitted by equations 4.3 and 4.4 (figure 5.2 d, e). In the case of $[Au_2(IPr)_2(PhCCCH_3)(OH)]^+$, the second isotopic peak was taken for analysis, because the first isotopic peak of the labeled ion overlaps with the fourth isotopic peak of the unlabeled ion. The obtained rate constants *k'* and half-lives of the ions $[Au(IPr)(PhCCCD_3)(H_2O)]^+$ and $[Au_2(IPr)_2(PhCCCD_3)(OH)]^+$ are presented in table 5.1 and table 5.2. Half-lives were calculated according to equation 4.5, rate constant *k'* corresponds to the rate of the ion decomposition. I set the estimated error of the determined rate constants as at least 10%. I usually obtain a smaller deviation of the determined values, but given all possible sources of the experimental errors I prefer to give a conservative estimation of the overall experimental error.

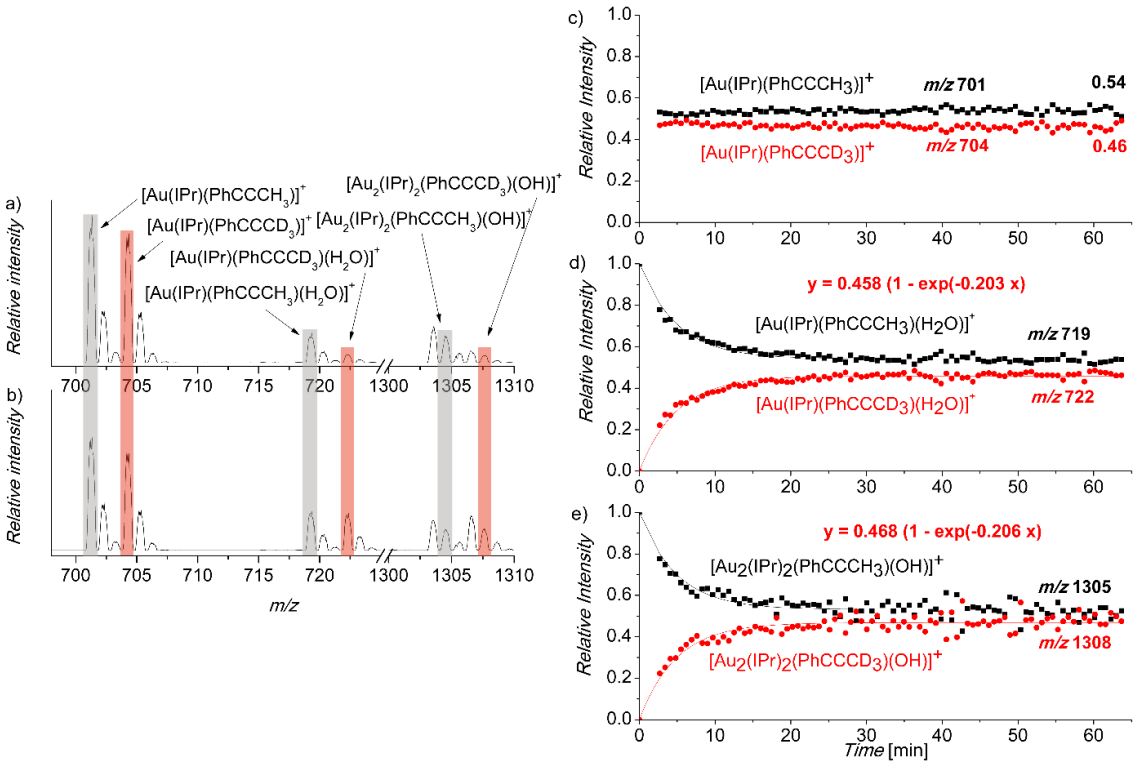

Figure 5.2. ESI-MS source spectra of the reaction mixture a) 2 minutes and b) 60 minutes after addition of stock solution C, which contains $PhCCCD_3$ (t_d = 1 hour). Graph c-e): time dependence of the relative intensities of the signals of the labeled and the unlabeled ions. The full curves represent the fits with equations 4.3 and 4.4.

From the results in table 5.1 and 5.2 is clear that the time delay in the interval that I have investigated has only a small influence on the obtained values (for the experimental curves see figure 5.3).

Table 5.1. Rate constants *k'* and half-lives of the $[Au(IPr)(PhCCCD_3)(H_2O)]^+$.

t_d	*k'* [min^{-1}]		$t_{1/2}$ [min]	
30 minutes	0,178	0,18 ± 0,02	3,9	4 ± 0,6
	0,176		3,9	
	0,178		3,9	
1 hour	0.203	0,17 ± 0,02	3,4	4 ± 0,7
	0,167		4,2	
	0,165		4,2	
	0,166		4,2	
	0,165		4,2	
2 hours	0,172	0,19 ± 0,02	4,0	4 ± 0,6
	0.204		3,4	
	0,184		3,8	

Table 5.2. Rate constants *k'* and half-lives for the $[Au_2(IPr)_2(PhCCCD_3)(OH)]^+$.

t_d	*k'* [min^{-1}]		$t_{1/2}$ [min]	
30 minutes	0,173	0,17 ± 0,02	4	4 ± 0,7
	0,173		4	
	0,173		4	
1 hour	0,206	0,18 ± 0,02	3,4	4 ± 0,6
	0,165		4,2	
	0,156		4,4	
	0,173		4	
	0,176		3,9	
2 hours	0,185	0,19 ± 0,02	3,7	4 ± 0,6
	0,193		3,6	
	0,205		3,4	

In the figure 5.3 a difference between relative intensities of ions $[Au(IPr)(PhCCCH_3)]^+$ and $[Au(IPr)(PhCCCD_3)]^+$ is noticeable. The experiments performed with 30 min and 1 hour delays show the slightly larger concentration of the unlabeled alkyne. This is clearly due to a somewhat smaller concentration of the labeled alkyne in the stock solution than that of the unlabeled alkyne. On contrary, the experiment with the 2 hours time delay (figure 5.3 g) shows a larger intensity of the signals originating from the labeled alkyne. The possible reason is that a considerable part of the unlabeled alkyne reacted during the time delay of this experiment, but the inaccuracy in the mixing of the solution cannot be excluded either.

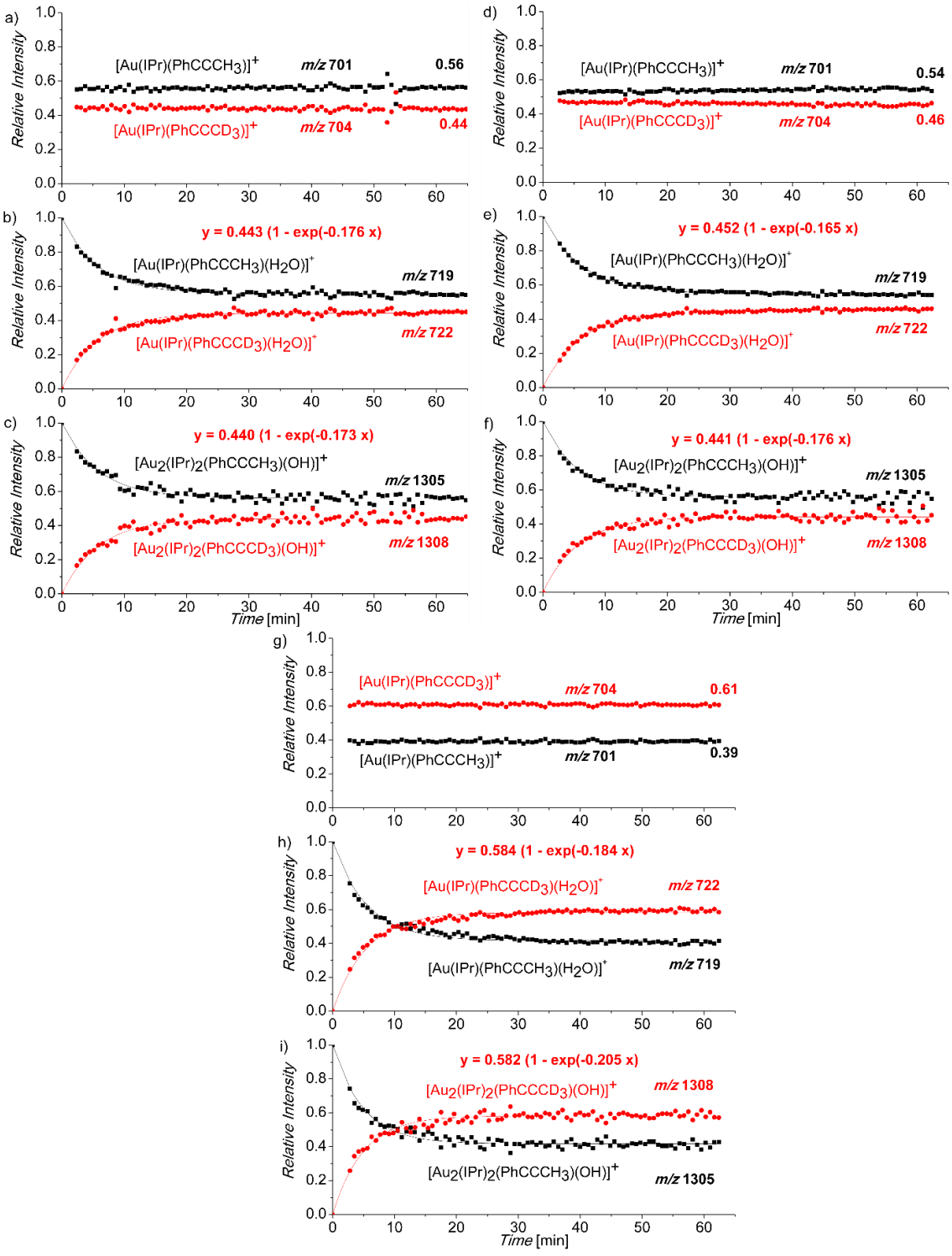

Figure 5.3. Time dependence of the relative intensities of the signals of the labeled and the unlabeled ions in the experiments with a different time delay: a-c) 30 minutes, d-f) 1hour, g-i) 2 hours. The full curves represent fits with equations 4.3 and 4.4.

b) Experiments with D_2O

Later I focused on the possible effect of using D_2O instead H_2O on the obtained rate constants. As the optimum time delay for those experiments I chose one hour. Capillary was washed with dry acetone and D_2O before measurement in order to avoid H/D exchange between reactants and chemicals adsorbed on the walls of the capillary.

Reaction mixtures were prepared under argon by mixing 80 µl of the stock solution A, 120 µl of B and 100 µl of D_2O in 200 µl of dry acetone (for composition of the stock solutions see table 6.1) and left to react for 1 hour. Stock solutions for this experiment were prepared under argon with dry acetone. After the time delay, 120 µl of solution C was added, and the reaction mixture was immediately monitored by ESI-MS.

The result of one of the experiments is shown in figure 5.4. Only a small signal of the ions $[Au_2(IPr)_2(PhCCCD_3)(OD)]^+$ and $[Au(IPr)(PhCCCD_3)(D_2O)]^+$ is in the spectrum recorded 9 minutes after the solution C was added (figure 5.4a). In the spectrum recorded 100 minutes after the mixing (figure 5.4b), the signal intensities of the ions $[Au_2(IPr)_2(PhCCCD_3)(OD)]^+$ and $[Au(IPr)(PhCCCD_3)(D_2O)]^+$ still does not achieve the ratio 1:1 with respect to the peaks of $[Au_2(IPr)_2(PhCCCH_3)(OD)]^+$ and $[Au(IPr)(PhCCCH_3)(D_2O)]^+$. As above, the equilibrium for a complex between the catalyst and the alkyne (figure 5.4c) is achieved fast so that it cannot be observed by the current technique.

Obtained rate constants *k'* and half-lives of the ions $[Au(IPr)(PhCCCH_3)(D_2O)]^+$ and $[Au_2(IPr)_2(PhCCCH_3)(OD)]^+$ are presented in table 5.3 and table 5.4. In the case of ions $[Au(IPr)(PhCCCH_3)(D_2O)]^+$ and $[Au_2(IPr)_2(PhCCCH_3)(OD)]^+$ the second isotopic peak was taken for the analysis, because the first isotopic peak of the labeled ion overlaps with the fourth isotopic peak of the unlabeled ion.

Table 5.3 Rate constants *k'* and half-lives of the $[Au(IPr)(PhCCCD_3)(D_2O)]^+$.

t_d	*k'* [min^{-1}]		$t_{1/2}$ min	
	0,029		23,9	
	0,036		19,3	
1 hour	0,033	0,033 ± 0,004	21,0	21 ± 4
	0,038		18,2	
	0,029		23,9	

Table 5.4 Rate constants *k'* and half-lives for the $[Au_2(IPr)_2(PhCCCD_3)(OD)]^+$.

t_d	k' [min^{-1}]		$t_{1/2}$ min	
	0,033		21,0	
	0,038		18,2	
1 hour	0,035	),035 ± 0,004	19,8	20 ± 3
	0,040		17,3	
	0,030		23,1	

The decrease of the obtained values compared to the experiments with H_2O is due to the kinetic isotope effect in the reaction. The following equation expresses the kinetic isotope effect (KIE):

$$KIE = \frac{k_H}{k_D}, \tag{5.1}$$

where k_H is the rate constant for a reaction with an unlabeled reactant and k_D is the rate constant for the reaction with the corresponding labeled reactant. The kinetic isotope effect for the degradation of $[Au(IPr)(PhCCCH_3)(D_2O)]^+$ is *KIE* = 5,3 ± 1 and for that of $[Au_2(IPr)_2(PhCCCH_3)(OD)]^+$ it is *KIE* = 5,0 ± 1.

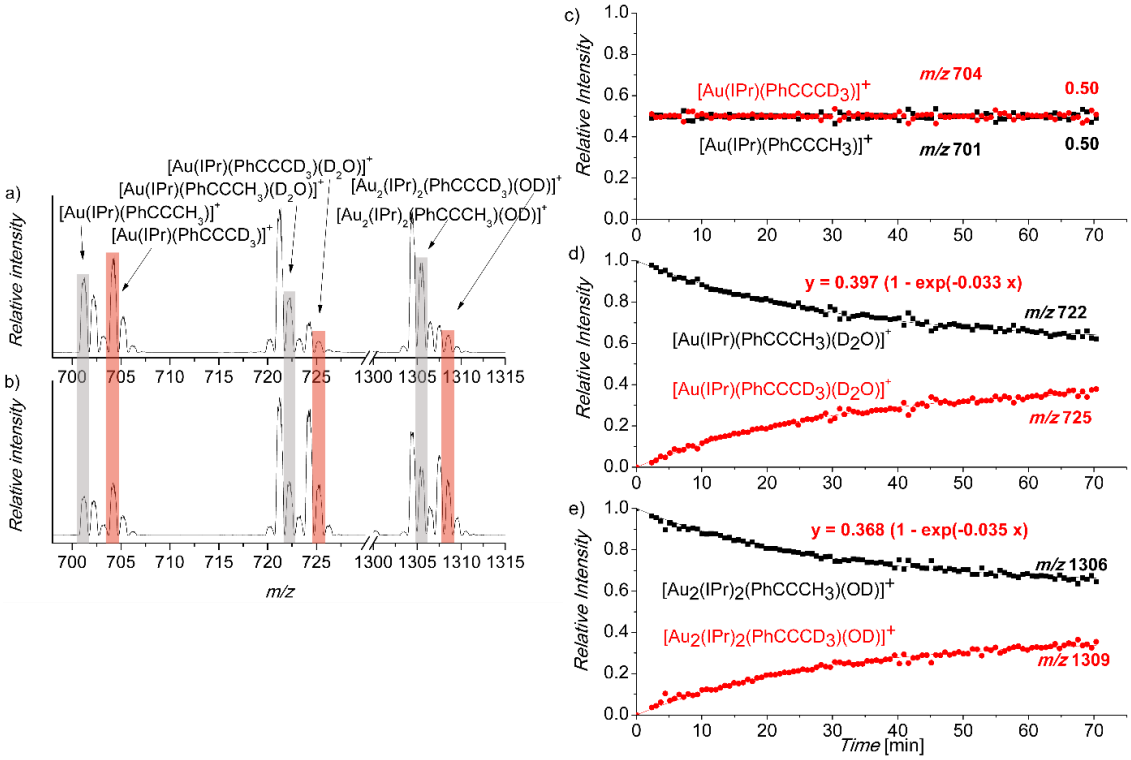

Figure 5.4. ESI-MS source spectra of the reaction mixture a) 9 minutes and b) 100 minutes after addition of the stock solution C, which contains $PhCCCD_3$ (t_d = 1 hour). Graph c-e): time dependence of the relative intensities of the signals of the labeled and the unlabeled ions. The full curves represent the fits with equations 4.3 and 4.4.

5.2 Labeling with D_2O

a) Experiments with D_2O and H_2O added to the reaction mixture at the same time

Reaction mixtures were prepared by mixing 80 µl of the stock solution A, 120 µl of B, 100µ of H_2O and 100 µl of D_2O in 200µl of acetone (for the composition of the stock solutions see table 6.1). After this, reaction mixtures were immediately monitored by ESI-MS.

The averaged ESI-MS spectrum is shown in figure 5.5 a. The time dependence of the normalized intensities of the signals of the labeled and the unlabeled peaks of ions $[Au(IPr)(H_2O)]^+$ (*m/z* = 603), $[Au(IPr)(PhCCCH_3)(H_2O)]^+$ (*m/z* = 719), $[Au_2(IPr)_2(OH)]^+$ (*m/z* = 1187) and $[Au_2(IPr)_2(PhCCCH_3)(OH)]^+$ (*m/z* = 1303) are shown in figure 5.5 b-e). Averages of the relative intensities of the signals of the labeled and the unlabeled peaks are given in table 5.5.

The monitored signals differ only by 1 Dalton (difference between H and D containing ions). The deuterium containing ions are isobaric with H-analogs that contain one ^{13}C isotope. I had to, therefore, account for this and correct the intensities of the observed signals. The signals intensities of the ions with *m/z* = 604 and *m/z* = 605 were corrected with respect to the natural isotope composition of the base peak *m/z* = 603. The signal intensity of the ions with *m/z* = 605 in addition was also corrected with respect to the natural isotope composition of the base peak at *m/z* = 604.The same approach was applied to the signals of the ions with *m/z* = 720, *m/z* = 721 and *m/z* = 1304. For the signals intensities of the ions with *m/z* = 603 and *m/z* = 604 a correction with respect to the natural isotope composition of the interfering ion $[Au(IPr)(NH_3)]^+$ with *m/z* = 602 was also required. This signal appeared occassionally and probably originated from some impurities in the used capillary.

Table 5.5. Average of the relative intensities of the signals of the labeled and the unlabeled peaks.

m/z = 603	*m/z* = 604	*m/z* = 605	*m/z* = 719	*m/z* = 720
0,40 ± 0,04	0,46 ± 0,05	0,14 ± 0,03	0,40 ± 0,04	0,53 ± 0,05
m/z = 721	*m/z* = 1187	*m/z* = 1188	*m/z* = 1303	*m/z* = 1304
0,07 ± 0,01	0,50 ± 0,05	0,50 ± 0,05	0,85 ± 0,08	0,15± 0,02

As we can see from the ratio of the signal abundances of the labeled and unlabeled ion $[Au_2(IPr)_2(OH)]^+$ (*m/z* = 1187), ratio of the added H_2O to D_2O is almost exactly 1:1 (figure 5.5 c). The results for $[Au(IPr)(H_2O)]^+$ and its isotopologs (*m/z* 603, 604, and 605) do not show the statistical ratio (i.e. 25 : 50 : 25 ratio would be expected). I assign this to the experimental artefact. The signal of these ions is very small and the applied corrections might disturb the final results. I will not consider these ions further, but I will list the results for the sake of completeness. The ratio of the signal abundances of the labeled and unlabeled ion $[Au_2(IPr)_2(PhCCCH_3)(OH)]^+$ (*m/z* = 1187) is 0,84 : 0,16. From knowing that I have prepared the reaction mixture with 1:1 ratio of H_2O to D_2O I can conclude, that the added H (D) is not acidic and therefore does not exchange with D (H) Hence, it is not bound to the oxygen atom, but it must be bound to a carbon atom. This also suggest that one of the $[Au(IPr)]^+$ cations is attached to a carbon atom and the other to the carbonyl oxygen (see discussion below).

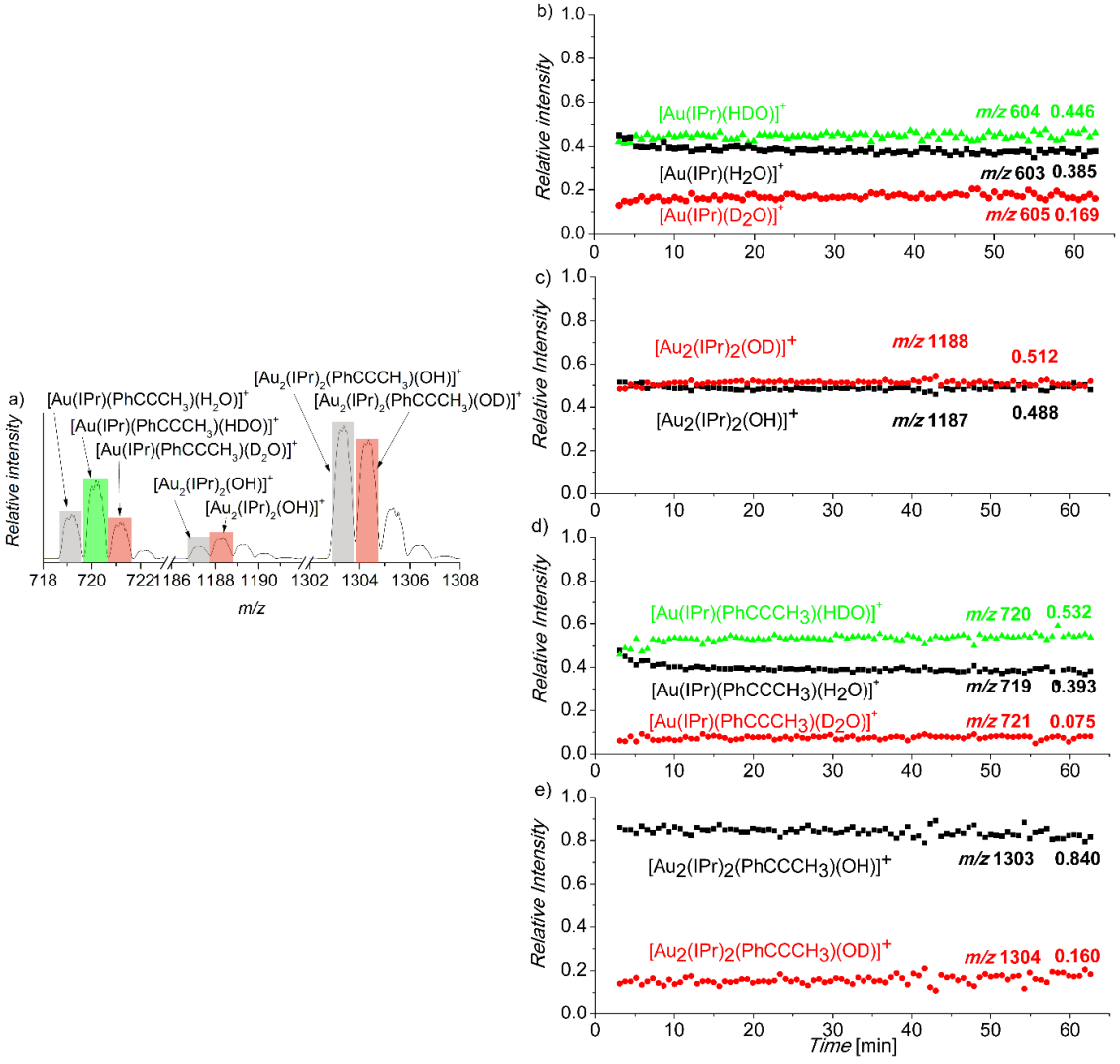

Figure 5.5. a) ESI-MS spectrum of the reaction mixture. Graphs b-e): time dependence of the relative intensities of the signals of the labeled and the unlabeled ions.

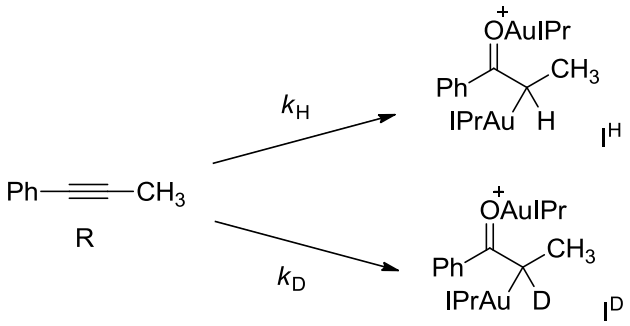

Scheme 5.1. Formation of the labeled and the unlabeled ion $[Au_2(IPr)_2(PhCCCH_3)(OH)]^+$.

From the signal abundances of the labeled and unlabeled ions $[Au_2(IPr)_2(PhCCCH_3)(OH)]^+$ I can express the kinetic isotope effect for the formation of $[Au_2(IPr)_2(PhCCCH_3)(OH)]^+$. If k_H is the rate constant for the formation of $[Au_2(IPr)_2(PhCCCH_3)(OH)]^+$ and k_D is the rate constant for the formation of $[Au_2(IPr)_2(PhCCCH_3)(OD)]^+$, $[I^H]$ is the concentration of the unlabeled intermediate, $[I^D]$ is the concentration of the labeled intermediate and [R] is the concentration of the reactant (scheme 5.1) I can derive following rate equations:

$$\frac{d[I^H]}{dt} = k_H[R] \tag{5.2}$$

$$\frac{d[I^D]}{dt} = k_D[R] \tag{5.3}$$

The integrated equations are then ($[R]_0$ is the concentration of the reactant at the beginning of the reaction):

$$[I^H] = \frac{k_H}{k_H+k_D}\,[R]_0(1 - e^{-(k_H+k_D)t}) \tag{5.4}$$

$$[I^D] = \frac{k_D}{k_H+k_D}\,[R]_0(1 - e^{-(k_H+k_D)t}) \tag{5.5}$$

According to equations 5.6 and 5.7 for kinetic isotope effect can be described as:

$$KIE = \frac{k_H}{k_D} = \frac{[I^H]}{[I^D]} \tag{5.6}$$

From the equation 5.6 the *KIE* for formation of ion $[Au_2(IPr)_2(PhCCCH_3)(OH)]^+$ is 5,6 ± 0,5.

Slightly more complicated situation is in the case of monoaurated intermediate. The signal of the peak with *m/z* = 720 corresponds to the ion $[Au(IPr)(PhCCCH_3)(DOH)]^+$. The relative signal abundance of this peak compared to $[Au(IPr)(PhCCCH_3)(D_2O)]^+$ and $[Au(IPr)(PhCCCH_3)(H_2O)]^+$ is 0,53 ± 0,05. If I would assume that only one of the two hydrogen atoms of the incoming water molecule is labile and undergoes hydrogen scrambling with water in solution (they are in 1:1 ratio), then I would expect exactly this result. The ratio of $[Au(IPr)(PhCCCH_3)(H_2O)]^+$ to $[Au(IPr)(PhCCCH_3)(D_2O)]^+$ gives us then the KIE for the addition of water to form the intermediate with one labile hydrogen atom (i.e. one of the hydrogen atoms is bound to a carbon atom, whereas the other one stays at the oxygen atom). The KIE for formation of the ion $[Au(IPr)(PhCCCH_3)(H_2O)]^+$ is 5,7 ± 0,4.

b) Experiments, where H_2O is added to the mixture first

Reaction mixtures were prepared by mixing 80 µl of the stock solution A, 120 µl of B and 100 µl of H_2O in 200µl of acetone (for the composition of the stock solutions see table 6.1) and left to react for a time delay. After a time delay elapsed, 100 µl of D_2O was added to the reaction mixture and it was immediately monitored by ESI-MS.

Three different time delays were tested: 30 minutes, 1 hour and 2 hours. The result of the experiment with the time delay 30 minutes is shown in figure 5.5. In spectra a) and b) a slow increasing of the intensities of the ions that contain deuterium is visible. As it was expected from the experiments mentioned above, the ratio of the signal abundances of the labeled and unlabeled ion $[Au_2(IPr)_2(PhCCCH_3)(OH)]^+$ is changing only very slowly.

For the analysis, the signal intensities were corrected for isotope impurities (as described in chapter 5.2.a) and the sum of the intensities of the signals of the labeled and the unlabeled peaks was normalized to 1. As you can see in figure 5.6 and 5.7, the time delay in the interval that I have investigated had only a small effect on the obtained experimental curves. The experiments cannot be evaluated as it was done for the labeling with $PhCCCD_3$, because the formations of the intermediates have different rates. Experiments are also compromised by the H/D scrambling of the monoaurated intermediates.

Nevertheless, I can evaluate the results qualitatively. Experiments show that kinetics of H/D scrambling at the monoaurated intermediate is slightly slower than the formation of $[Au_2(IPr)_2(OD)]^+$, but much faster than the kinetics associated with the formation of diaurated intermediate. If we look at the $[Au_2(IPr)_2(PhCCCH_3)(OD)]^+$ and

[Au(IPr)(PhCCCH$_3$)(D$_2$O)]$^+$ signals, we can notice that the behavior of the mono- and the diaurated intermediates are very similar as already established in the experiments above.

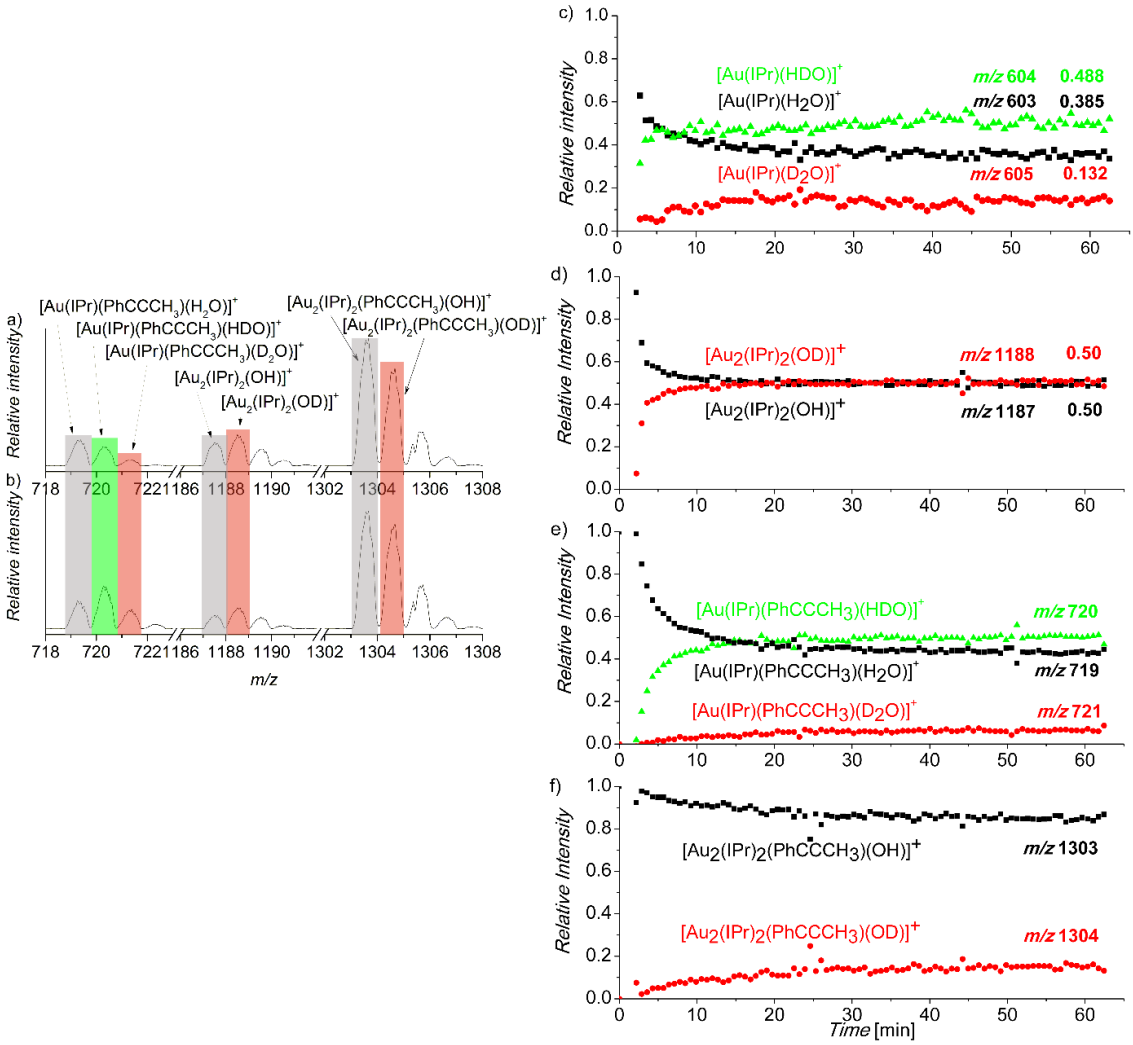

Figure 5.6. ESI-MS source spectra of the reaction mixture a) 3 minutes and b) 60 minutes after addition of D_2O (t_d = 30 minutes). Graphs c-e): time dependence of the relative intensities of the signals of the labeled and unlabeled ions.

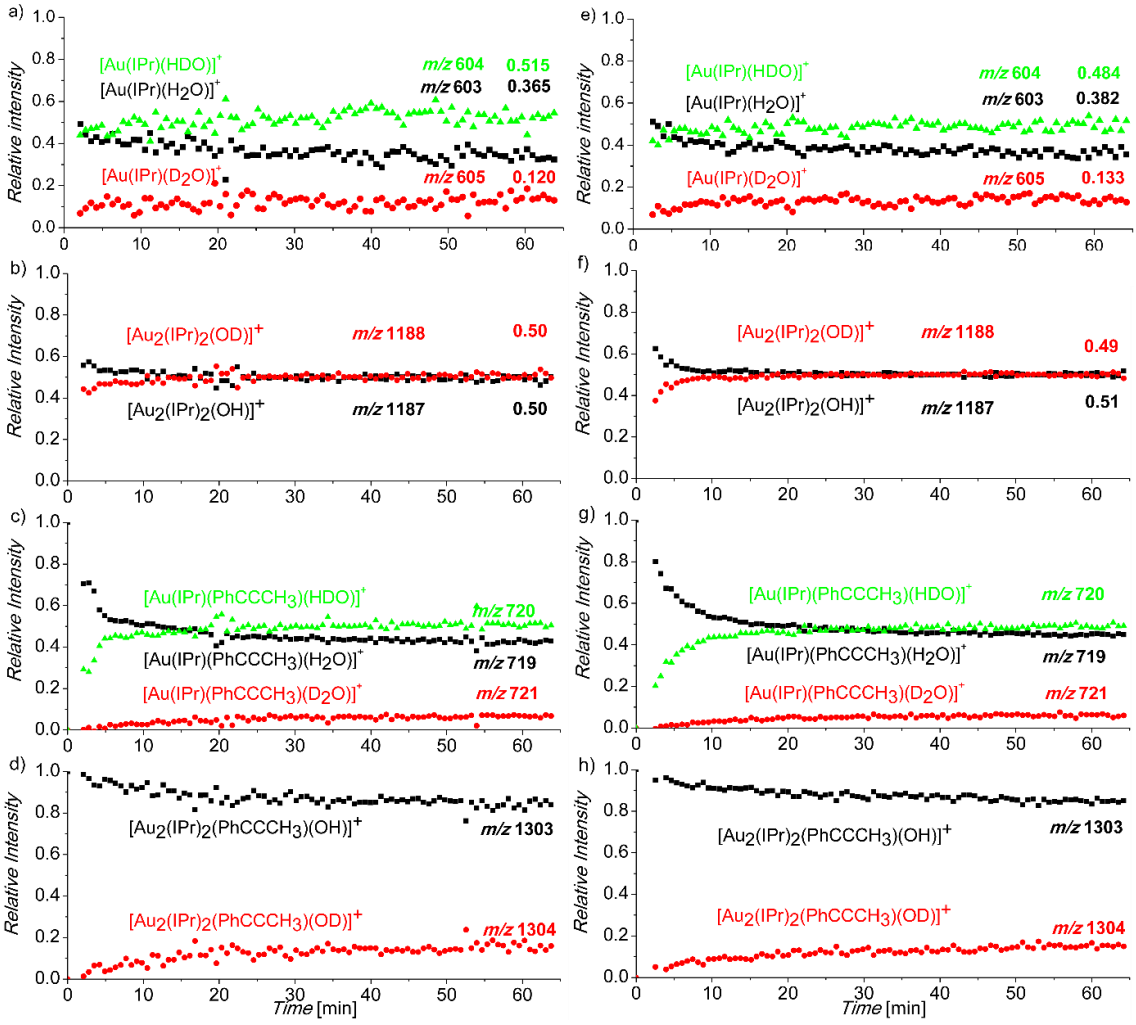

Figure 5.7. Time dependence of the relative intensities of the signals of the labeled and unlabeled ions (a-d: t_d = 1 hour, e-h: t_d = 2 hours).

c) Experiments where D_2O is added to the reaction mixture first

The reaction mixtures were prepared under argon with dry acetone by mixing 80 µl of the stock solution A, 120 µl of B and 100 µl of D_2O in 200µl of acetone (for the composition of the stock solutions see table 6.1) and left to react for a time delay. After the time delay elapsed, 100 µl of H_2O was added to the reaction mixture and it was immediately monitored by ESI-MS.

The result of the experiment with the time delay 30 minutes is shown in figure 5.8. In spectra a) and b) rapid increasing of the intensities of the ions that contain H is visible.

For the analysis, the signal intensities were corrected for the isotope impurities (as described in chapter 5.2.a) and the sum of the intensities of the signals of the labeled and the unlabeled peaks was normalized to 1. Three different time delays were tested: 30 minutes, 1 hour and 2 hours. The time delay in the interval that I have investigated has only a small effect on the obtained experimental curves. Experiments cannot be evaluated as for labeling with $PhCCCD_3$, because the formations of the intermediates have different rates.

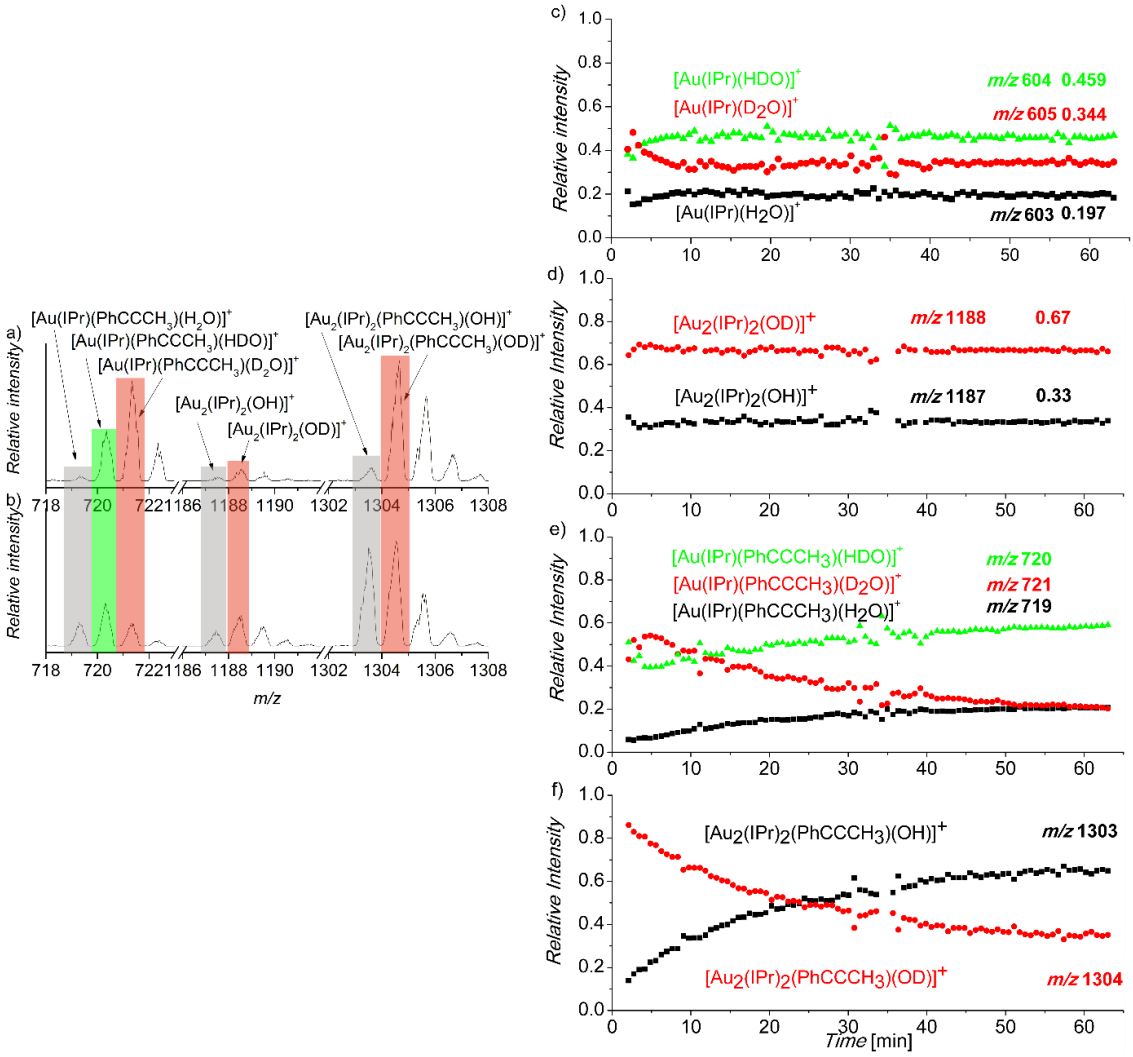

Figure 5.8. ESI-MS source spectra of the reaction mixture a) 6 minutes and b) 100 minutes after addition of H_2O (t_d = 1 hour). Graphs c-e): time dependence of the relative intensities of the signals of the labeled and the unlabeled ions. Full curves represent fits with equations 4.3 and 4.4.

5.3 NMR

We started measurement using the reaction mixture without the catalyst. The mixture was prepared by mixing 240 µl of B and 100 µl of H_2O in 200µl of D_6-acetone (for the composition of the stock solutions see table 6.1). Then, 80 µl of the stock solution A was added and the reaction mixture was immediately studied by NMR. Examples of ^1H NMR spectra are shown in figure 5.9. Peaks labeled with black stars belong to the catalyst and their intensities do not change during the reaction. The peak labeled with the red star was in the mixture already before the catalyst was added and its intensity does not change during reaction.

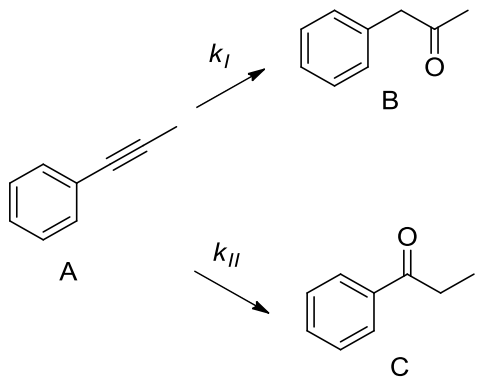

Scheme 5.2. Addition of water to phenylpropyne.

Based on scheme 5.2 following differential equations were suggested:

$$\frac{d[A]}{dt} = -k_I[A] - k_{II}[A], \quad (5.7)$$

$$\frac{d[B]}{dt} = k_I[A], \quad (5.8)$$

$$\frac{d[C]}{dt} = k_{II}[A]. \quad (5.9)$$

These equations were used as a kinetic model for fitting experimental data with mathematic software GNU Octave.[50] Rate constants k_I and k_{II} were free fit parameters, equations were solved numerically, fitting was performed with the least squares method. Obtained rate constants are shown in table 5.6, fits of the experimental data are in figure 5.10.

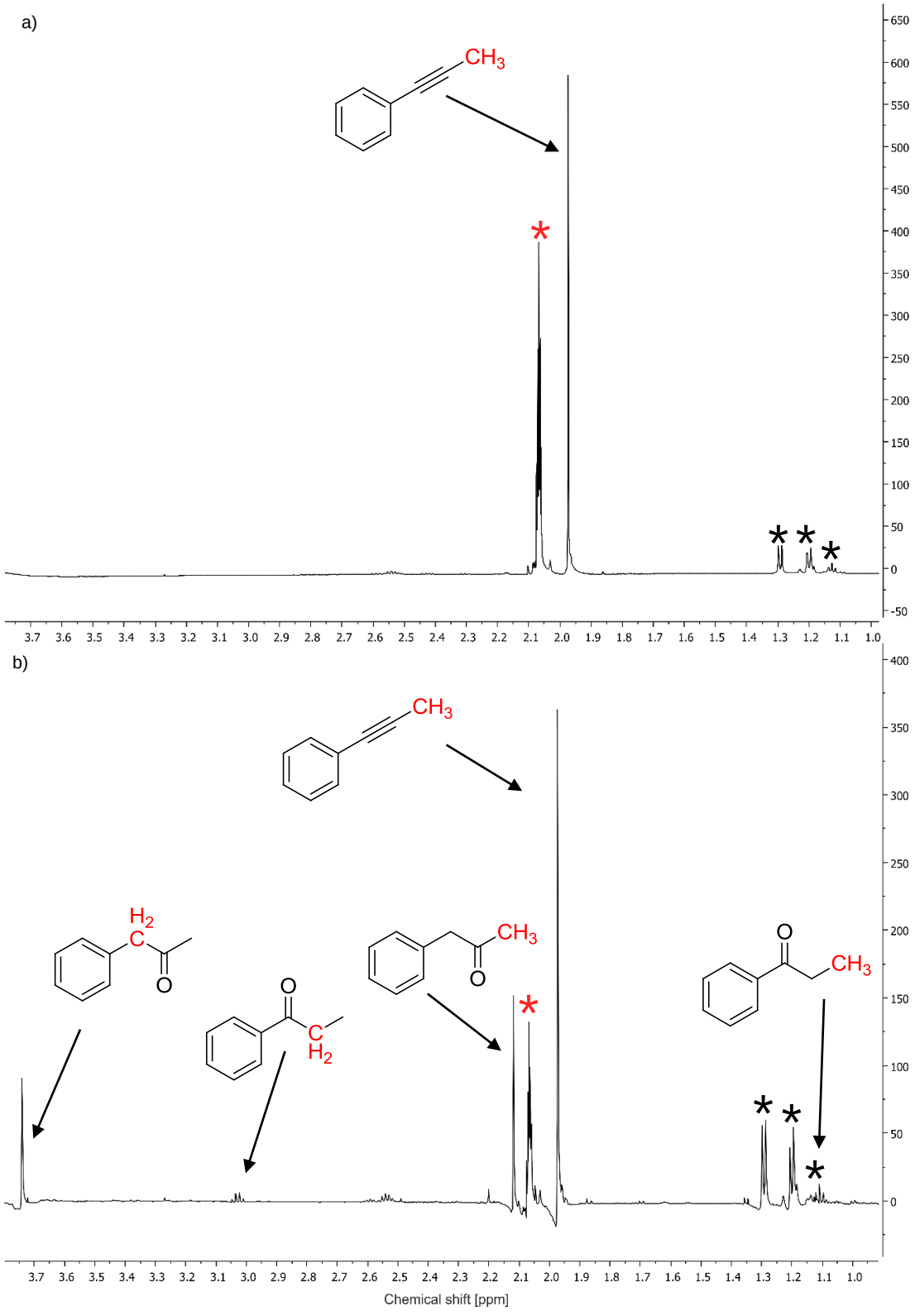

Figure 5.9. ^{1}H NMR spectrum of the reaction mixture a) 3 minutes after the catalyst was added, a) 200 minutes after the catalyst was added. All signals correspond to the red labeled methyl group.

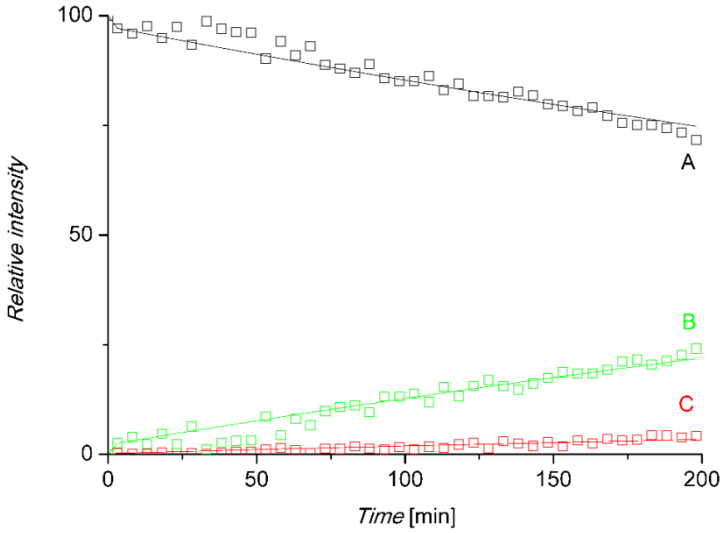

Figure 5.10. The relative ratio of 1-phenyl-1-propyne (A), phenylacetone (B) and propiophenone (C). Full curves represent the kinetic fits obtained by GNU Octave.

Table 5.6. Rate constants obtained by NMR spectroscopy.

k_I^{NMR} [min^{-1}]	k_{II}^{NMR} [min^{-1}]
$12 \cdot 10^{-4}$	$1{,}86 \cdot 10^{-4}$

Thus, the overall rate constant from the kinetic modeling for the hydration od 1-phenyl-1-propyne catalyzed by gold complex $[Au(IPr)(MeCN)]BF_4$ is $13{,}86 \cdot 10^{-4}$ min^{-1} ($0{,}815$ $dm^3 \cdot mol^{-1} \cdot min^{-1}$). Phenylacetone is formed with a larger rate constant and prevails in the reaction mixture over the alternative product propiophenone.

5.4 Discussion

The NMR data for hydration of 1-phenyl-1-propyne catalyzed by gold complex $[Au(IPr)(MeCN)]BF_4$ shows that phenylacetone prevails in the reaction mixture over the alternative product propiophenone. The overall rate constant from the kinetic modeling for this reaction is $1{,}386 \cdot 10^{-3}$ min^{-1} (0,815 $dm^3 \cdot mol^{-1} \cdot min^{-1}$). The reaction is very slow (the concentrations of the reactants are changing only very slowly with respect to the time of the experiment), so the requirements for the kinetic modeling of the mass spectrometry data are fulfilled.

Delayed reactant labeling of $[Au(IPr)(PhCCCH_3)(H_2O)]^+$ shows a clear behavior of intermediate because the shapes of the curves representing the relative abundances of the unlabeled and the labeled signals correspond to the establishment of steady-state conditions.

From the experiments with labeled phenylpropyne I have obtained the kinetic isotope effects for ions decomposition of detected intermediates. *KIE* = 5,3 ± 1 for $[Au(IPr)(PhCCCH_3)(H_2O)]^+$ and for $[Au_2(IPr)_2(PhCCCH_3)(OH)]^+$ *KIE* = 5,0 ± 1.

The experiments where D_2O and H_2O were added to mixture at the same time shows that the hydrogen atom in $[Au_2(IPr)_2(PhCCCH_3)(OH)]^+$ is bound to a carbon atom and that one of the $[Au(IPr)]^+$ cations is attached to a carbon atom and the other to the carbonyl oxygen. This experiment also shows that one of hydrogen atoms in $[Au(IPr)(PhCCCH_3)(H_2O)]^+$ is scrambling.

From this experiment, I obtained the *KIE* for the formation of the ion $[Au_2(IPr)_2(PhCCCH_3)(OH)]^+$ as 5,6 ± 0,5 and *KIE* for the formation of the ion $[Au(IPr)(PhCCCH_3)(H_2O)]^+$ as 5,7 ± 0,4, which clearly demonstrated that the rate determining step for the formation of both intermediates is connected with a hydrogen rearrangement.

The experiments where D_2O and H_2O were added to the mixture with a time delay are compromised by the H/D scrambling for the monoaurated intermediates. Nevertheless, I evaluated the results qualitatively.

The experiments show the kinetics of H/D scrambling. If D_2O is added with a delay to the reaction mixture containing H_2O, I can clearly follow the relatively fast formation of $[Au_2(IPr)_2(OD)]^+$ and somewhat slower H/D scrambling at the monoaurated intermediate. If H_2O is added with a delay to the reaction mixture containing D_2O, the formation of $[Au_2(IPr)_2(OH)]^+$ as well as the H/D scrambling at the monoaurated intermediate are so

fast that we cannot follow it with our technique. This once more demonstrates KIE associated with all reactions observed.

On the basis of all experimental data (rate constants and kinetic isotope effect) I conclude, that monoaurated and diaurated ions have the same kinetics of degradation. This is most probably because the degradation corresponds to protodeauration of analogous carbon atoms in both cases (see scheme 5.3).

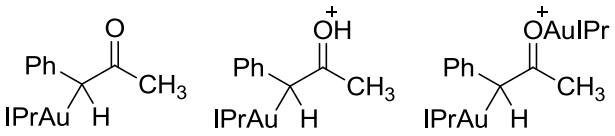

Scheme 5.3. Possible structures of the intermediates.

Surprisingly, I have also similar results for the kinetics of the formation of the mono- and diaurated intermediates. Again, the same KIE was found. We were not able to extract the quantitative data for the rate constants for the intermediate formations (the experiments with delayed labeling with either D_2O or H_2O). Nevertheless, qualitatively, the kinetics appear again the same. Possible explanation is that the diaurated and protonated ions might be formed during electrospray process by trapping neutral intermediate by either gold cation or proton. This would mean that both signals, in fact, monitor one neutral intermediate present in solution. Possible structures of the intermediates are in scheme 5.3. An alternative explanation involves addition of $[Au_2(IPr)_2(OH)]^+$ which would primarily lead to the diaurated intermediate. The diaurated intermediate can than undergo protodeauration to form the monoaurated intermediate or simply provides the neutral monoaurated intermediate that is sampled by ESI as protonated ion.

In the following, I will suggest alternative mechanisms consistent with the findings above. The first possibility is shown in scheme 5.4.

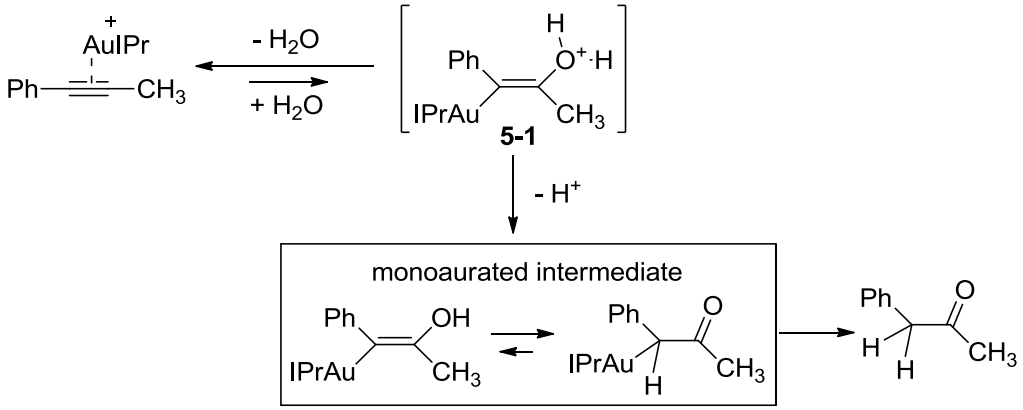

Scheme 5.4. A possible mechanism of the formation of the neutral intermediate.

The first reversible step is the addition of water to a gold-activated phenylpropyne. The next step is deprotonation of **5-1** yielding the monoaurated intermediate. The equilibrium is shifted to the keto-form of the intermediate. The monoaurated intermediate then decomposes through protodeauration to the product. Alternatively, the addition can proceed via dual activation (Scheme 5.5). Instead of the water addition, the reaction would be mediated by $[Au_2(IPr)_2(OH)]^+$. One gold cation then activates the triple bond, whereas the other stays at the oxygen atom and makes the addition strongly exothermic.[23,27]

For the comparison of the rate constants obtained in ESI-MS experiments with rate constants obtained in NMR experiment, it is important to consider concentration of the reactive intermediates. Hence, the average rate constant for the decomposition of the intermediates is $0{,}18 \pm 0{,}02$ min^{-1}. The concentration of the gold catalyst is 5 mol% with respect to the alkyne reactant that is followed in the NMR experiment. If 100% of the present gold catalyst would be active in the reaction, then the expected overall rate constant for the reaction, where protodeauration of the intermediate is the rate determining step, would be $9 \cdot 10^{-3}$ min^{-1}. The value from the NMR experiment is $1{,}4 \cdot 10^{-3}$ min^{-1}. Clearly, not all gold cations are bound in the intermediates and I detected a substantial amount of the diaurated ions. Therefore, the predicted maximum rate based on the MS experiment is in a very good agreement with the NMR data and I can conclude that my results are consistent with protodeauration being the rate determining step in this reaction

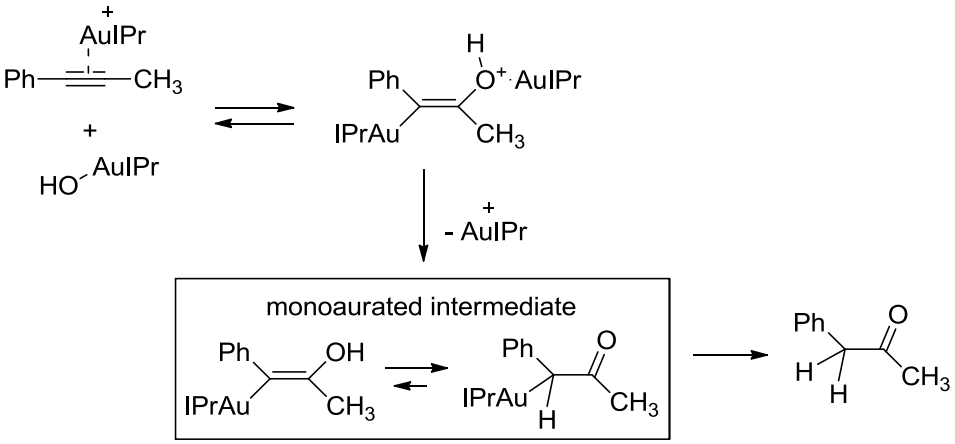

Scheme 5.5. Mechanism with a dual activation.

6 Experimental details

6.1 Electrospray ionization mass spectrometry

The main method that I used in my thesis was electrospray ionization mass spectrometry (ESI-MS). For my experiments I used Finnigan TSQ 7000 mass spectrometer with QOQ (Q – quadrupole, O – octopole) configuration (Scheme 6.1).

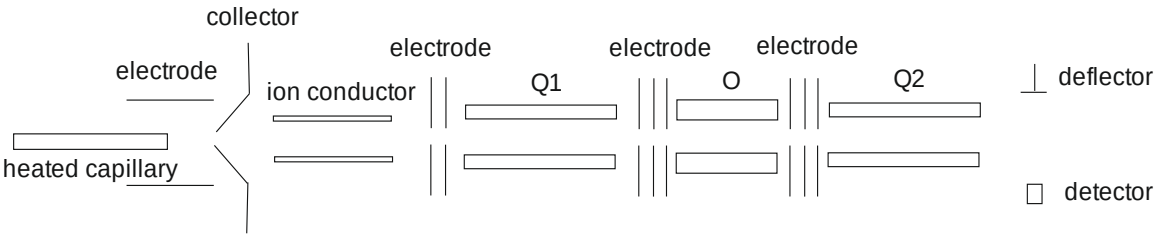

Scheme 6.1 Scheme of the Finnigan TSQ 7000 mass spectrometer.

Ions are generated by electrospray ionization source (Scheme 6.2). In the process, a sample is pumped through the capillary to the ESI source. Then, under high voltage, a spray of small droplets is formed. Droplets are subsequently desolved and transported through a heated capillary into a vacuum. Flow rate for the experiments was 0,3 $ml \cdot h^{-1}$. An input voltage was 4,5 kV. Nitrogen was used as a nebulizer gas. The pressure of nitrogen was adjusted according to the signal and was always in the range between 69 kPa and 207 kPa.

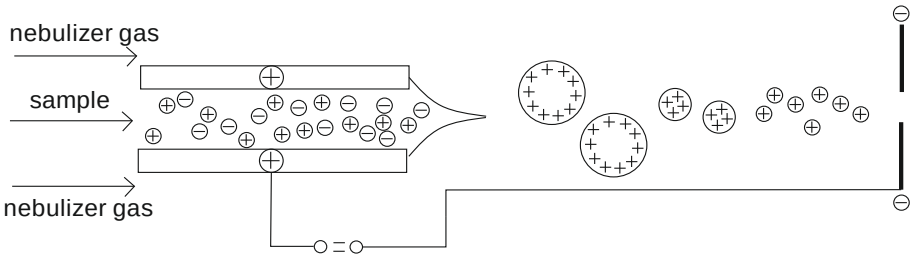

Scheme 6.2 Electrospray ionization process.

6.2 Nuclear magnetic resonance spectroscopy

NMR spectra were measured on Varian NMR System 600 MHz in $(CD_3)_2CO$ solution. For processing of data the program MestReNova was used. For numerical solution of the differential equations for the kinetic model and the fitting of the experimental data was used program CNU Octave.[54]

6.3 Chemicals

Complex [Au(IPr)MeCN]BF_4 and $PhCCCH_3$ were purchased from Sigma-Aldrich and used without further purification. Deuterated solvents were purchased from Acros Organics.

$PhCCCD_3$ was prepared in our lab according to scheme 6.3.[55]

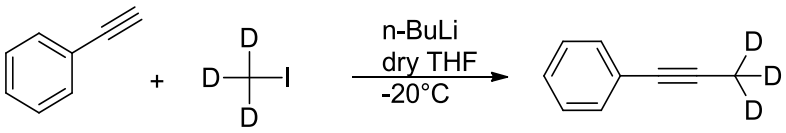

Scheme 6.3. Preparation of the 1-phenyl-1-propyn-3,3,3,-d_3.

6.4 Preparation of reaction mixtures for ESI-MS and NMR experiments

The general scheme for experimental setting is shown in scheme 6.4.

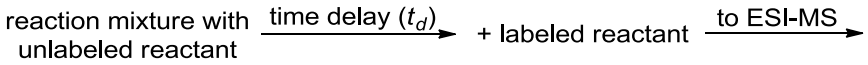

Scheme 6.4 General scheme of the experiments.

Reaction mixtures were prepared from the stock solutions. Table 6.1 shows the content of the stock solutions. For experiments, in which D_2O was added to the mixture first, stock solutions were prepared with dry acetone under argon. Stock solutions for NMR experiments were prepared using D_6-acetone.

Table 6.1. Contents of the stock solutions.

Solution	Reagent	Quantity	*n* / μmol	Solvent	Quantity
A	[Au(IPr)(MeCN)]BF_4	9.3 mg	13	Acetone	1 ml
B	$PhCCCH_3$	10 μl	80	Acetone	1 ml
C	$PhCCCD_3$	10 μl	80	Acetone	1 ml

7 Conclusion

The experiments proved that hydration catalyzed by gold complex $[Au(IPr)]^+$ proceeds via monoaurated intermediates. Monoaurated intermediates were detected by ESI-MS as protonated or aurated ions. From the obtained results it was clear that $[Au(IPr)]^+$ is bound to a carbon atom.

The obtained rate constants and half-lives from the experiments with labeled phenylpropyne are the same for both detected ions ($[Au(IPr)(PhCCCH_3)(H_2O)]^+$ and $[Au_2(IPr)_2(PhCCCH_3)(OH)]^+$). The KIEs for the decomposition of the intermediates were determined as *KIE* = 5,3 ± 1 for $[Au(IPr)(PhCCCH_3)(H_2O)]^+$ and for $[Au_2(IPr)_2(PhCCCH_3)(OH)]^+$ *KIE* = 5,0 ± 1. The obtained kinetic isotope effects are associated with protodeauration of $[AuIPr]^+$ bound to the carbon atom.

From the experiments where D_2O and H_2O were added to the reaction mixture at the same time I have determined *KIE*s for the formation of intermediates. The *KIE* for the formation of the ion $[Au_2(IPr)_2(PhCCCH_3)(OH)]^+$ is 5,6 ± 0,5 and *KIE* for formation of the ion $[Au(IPr)(PhCCCH_3)(H_2O)]^+$ is 5,7 ± 0,4. Surprisingly, the addition of $[(IPr)AuOH]^+$ that is associated with hydrogen rearrangement to the carbon atom has very similar KIE as the protodeauration reaction.

On the basis of present experimental data mechanism of the formation of the intermediate cannot be determined conclusively. For complete resolution of the mechanism of hydration of 1-phenyl-1-propyne catalyzed by gold complex $[Au(IPr)(MeCN)]BF_4$ additional experiments are required. Experiments with different counter ions, different concentrations of the catalyst and reactants might be useful for further investigation.

8 References

(1) Fürstner, A.; Davies, P. W. *Angew. Chemie - Int. Ed.* **2007**, *46*, 3410-3449.

(2) Hashmi, K., S., A. *Angew. Chemie, Int. Ed.* **2010**, *49*, 5232–5241.

(3) Muzart, J. *Tetrahedron* **2008**, *64*, 5815-5849.

(4) Banerjee, S.; Mazumdar, S. *Int. J. Anal. Chem.* **2012**, *2012*, 1–40.

(5) Jašíková, L.; Anania, M.; Hybelbauerová, S.; Roithová, J. *J. Am. Chem. Soc.* **2015**, *137*, 13647–13657.

(6) Hashmi, K., S., A. *Chem. Rev.* **2007**, *107*, 3180–3211.

(7) Gorin, D. J.; Toste, F. D. *Nature* **2007**, *446*, 395–403.

(8) Teles, J. H. *Angew. Chemie, Int. Ed.* **2015**, *54* , 5556–5558.

(9) de Frémont, P.; Singh, R.; Stevens, E. D.; Petersen, J. L.; Nolan, S. P. *Organometallics* **2007**, *26*, 1376–1385.

(10) Sromek, A. W.; Rubina, M.; Gevorgyan, V. *J. Am. Chem. Soc.* **2005**, *127*, 10500–10501.

(11) Dorel, R.; Echavarren, A. M. *Chem. Rev.* **2015**, *115*, 9028–9072.

(12) Marion, N.; Ramón, R. S.; Nolan, S. P. *J. Am. Chem. Soc.* **2009**, *131*, 448–449.

(13) Xu, Y.; Hu, X.; Shao, J.; Yang, G.; Wu, Y.; Zhang, Z. *Green Chem.* **2015**, *17*, 532–537.

(14) Xu, Y.; Hu, X.; Zhang, S.; Xi, X.; Wu, Y. *ChemCatChem* **2016**, *8*, 262–267.

(15) Nun, P.; Ramón, R. S.; Gaillard, S.; Nolan, S. P. *J. Organomet. Chem.* **2011**, *696*, 7–11.

(16) Veenboer, R. M. P.; Dupuy, S.; Nolan, S. P. *ACS Catal.* **2015**, *5*, 1330–1334.

(17) Teles, J., H. Hydration and Hydroalkoxylation of CC Multiple Bonds. In *Modern Gold Catalyzed Synthesis*, Hashmi A. S., K.; Toste, F., D.; Wiley-VCH Verlag & Co. KGaA, Boschstr. 12, 69469 Weinheim, Germany, 2012; 201-236.

(18) Parr, E. J. W.; Thomas, C. B.; Norman, R. *J. Chem. Soc. Perkin Trans. 1* **1976**, *833*, 1983–1987.

(19) Teles, J. H.; Brode, S.; Chabanas, M. *Angew. Chemie, Int. Ed.* **1998**, *37*, 1415–1418.

(20) Yang, W.; Hashmi A. S., K. *Chem. Soc. Rev.* **2014**, *43*, 2941–2955.

(21) Jiménez-Núñez, E.; Echavarren, A. M. *Chem. Rev.* **2008**, *108*, 3326–3350.

(22) Fustner, A. *Chem. Soc. Rev.* **2009**, *38*, 3208–3221.

(23) Roithová, J.; Janková, Š.; Jašíková, L.; Váňa, J.; Hybelbauerová, S. *Angew. Chemie, Int. Ed.* **2012**, *51*, 8378–8382.

(24) Oonishi, Y.; Gómez-Suárez, A.; Martin, A. R.; Nolan, S. P. *Angew. Chemie, Int. Ed.* **2013**, *52*, 9767–9771.

(25) Zhdanko, A.; Maier, M. E. *Chem. Eur. J.* **2014**, *20*, 1918–1930.

(26) Zhdanko, A.; Maier, M. E. *ACS Catal.* **2014**, *4*, 2770–2775.

(27) Gómez-Suárez, A.; Oonishi, Y.; Martin, A. R.; Vummaleti, S. V. C.; Nelson, D. J.; Cordes, D. B.; Slawin, A. M. Z.; Cavallo, L.; Nolan, S. P.; Poater, A. *Chem. Eur. J.* **2016**, *22*, 1125–1132.

(28) Fernández, G. A.; Chopa, A. B.; Silbestri, G. F. *Catal. Sci. Technol.* **2016**, *6*, 1921–1929.

(29) Ebule, R. E.; Malhotra, D.; Hammond, G. B.; Xu, B. *Adv. Synth. Catal.* **2016**, *358*, 1478–1481.

(30) Trinchillo, M.; Belanzoni, P.; Belpassi, L.; Biasiolo, L.; Busico, V.; D'Amora, A. *Organometallics* **2016**, *35* , 641–654.

(31) Ciancaleoni, G.; Belpassi, L.; Zuccaccia, D.; Tarantelli, F.; Belanzoni, P. *ACS Catal.* **2015**, *5*, 803–814.

(32) Goodwin, J. A.; Aponick, A. *Chem. Commun* **2015**, *51*, 8730–8741.

(33) Gaskell, S. J. *J. Mass Spectrom.* **1997**, *32*, 677–688.

(34) Roithová, J. *Chem. Soc. Rev.* **2012**, *41*, 547–559.

(35) Henderson, W.; Mcindoe, J. S. *Compr. Coord. Chem. II* **2003**, *2*, 387–391.

(36) Schulz, J.; Shcherbachenko, E.; Roithová, J. *Organometallics* **2015**, *34*, 3979–3987.

(37) Schulz, J.; Jašíková, L.; Škríba, A.; Roithová, J. *J. Am. Chem. Soc.* **2014**, *136*, 11513–11523.

(38) Roach, B.; Forgan, R.; Tasker, P. *Dalt. Trans.* **2010**, *39*, 5614–5616.

(39) Vikse, K. L.; Henderson, M. a; Oliver, A. G.; McIndoe, J. S. *Chem. Commun.* **2010**, *46*, 7412–7414.

(40) Zins, E. L.; Pepe, C.; Schröder, D. *J. Mass Spectrom.* **2010**, *45*, 1253–1260.

(41) Chen, P. *Angew. Chemie, Int. Ed.* **2003**, *42*, 2832–2847.

(42) Adlhart, C.; Chen, P. *Helv. Chim. Acta* **2000**, *83*, 2192–2196.

(43) Kim, Y. M.; Chen, P. *Int. J. Mass Spectrom.* **1999**, *185*, 871–881.

(44) Putau, A.; Brand, H.; Koszinowski, K. *J. Am. Chem. Soc.* **2012**, *134*, 613–622.

(45) Yunker, L. P. E.; Stoddard, R. L.; McIndoe, J. S. *J. Mass Spectrom.* **2014**, *49*, 1–

8.

(46) Kou, Y.; Nabetani, Y.; Masui, D.; Shimada, T.; Takagi, S.; Tachibana, H.; Inoue, H. *J. Am. Chem. Soc.* **2014**, *136*, 6021–6030.

(47) Li, W.; Wang, J. *Angew. Chemie, Int. Ed.* **2014**, *53*, 14186–14190.

(48) Thoen, K. K.; Smith, R. L.; Nousiainen, J. J.; Nelson, E. D.; Kenttamaa, H. I. *J. Am. Chem. Soc.* **1996**, *118*, 8669–8676.

(49) McIndoe, J. S.; Farrer, N. J. *Int. J. Mass Spectrom.* **2000**, *200*, 387–401.

(50) Schröder, D. *Acc. Chem. Res.* **2012**, *45*, 1521–1532.

(51) Paul Kebarle, U. H. V. *Mass Spectrom. Rev.* **2009**, *28*, 898–917.

(52) Agrawal, D.; Schröder, D. *Organometallics* **2011**, *30*, 32–35.

(53) Meert, P.; Govaert, E.; Scheerlinck, E.; Dhaenens, M.; Deforce, D. *Proteomics* **2014**, *16*, 1–26.

(54) S. H. John Eaton, David Bateman, R. W. *J. Chem. Inf. Model.* **2013**, *53*, 1689–1699.

(55) Arrowsmith, H. C.; Kresge, A. J. *J. Am. Chem. Soc.* **1986**, *108*, 7918–7920.